



GEM-Forest: A Global satellite EMbedding–based map of forests and tree crops for 2020

Daniel Paluba¹, Valerio Marsocci², Katarína Onačillová³, Yarin T. Puerta Quintana⁴, Adam Hastie^{4,5}

¹Department of Applied Geoinformatics and Cartography, Faculty of Science, Charles University, Prague, 128 00, Czechia

5 ²Φ-lab, European Space Agency (ESA/ESRIN), Frascati, 000 44, Italy

³Institute of Geography, Faculty of Science, Pavol Jozef Šafárik University in Košice, Košice, 040 01, Slovakia

⁴Department of Physical Geography and Geocology, Faculty of Science, Charles University, Prague, 128 00, Czechia

⁵Department of Botany, Faculty of Science, Charles University, Prague, 128 00, Czechia

Correspondence to: Daniel Paluba (daniel.paluba@natur.cuni.cz)

10 **Abstract.** The advent of big data in Earth Observation (EO), coupled with recent advances in Artificial Intelligence, has led to the development of geospatial embeddings that are compact, information-rich feature vectors designed to be ready-to-use in machine learning (ML) applications for a wide range of downstream tasks, including forest monitoring. Motivated by the limitations of existing global forest products and by policy requirements such as the EU Deforestation Regulation (EUDR), we assess whether lightweight classifiers applied to satellite embeddings from the Google DeepMind Alpha Earth Foundation (AEF) can accurately map global forest and tree crop extents. In this study, we introduce GEM-Forest, a global satellite embedding–based forest dataset in 10 m spatial resolution for 2020, and its associated products: GEM-FnF2020, a forest / non-forest (F/nF) classification, and GEM-TC2020, which further distinguishes non-forest areas containing tree crops. Using ~47,000 globally distributed training samples covering all major biomes, collected through an automated approach combining multiple forest-related, land cover and tree crop datasets, we compared multiple ML approaches ranging from linear models to neural networks. Accuracy assessment on a global F/nF dataset with ~21,000 samples showed similar performance across classifiers, with overall accuracies of 90–92% and macro F1-scores of 0.89–0.90, while linear models often outperformed more complex approaches. The validation of the tree crop subclass across 10 datasets showed larger differences among different ML models, with the highest accuracies achieved mostly by linear models. This consistency indicates that the embeddings encode highly informative and linearly separable structure for global F/nF discrimination, including tree-crop separation. A linear Support Vector Machine was therefore used to generate GEM-FnF2020 that achieves a 91% overall accuracy, a macro F1-score of 0.90, with balanced omission and commission error rates for forests (15% and 13%, respectively). These results match or exceed existing global products, with most errors occurring in open forests and forest–shrubland transition zones. Residual misclassifications of tree crops as forests in GEM-FnF2020 ranged from 0.5% to 14.8%, which demonstrates the importance of including the tree crop subclass in the GEM-TC2020 map. The GEM-TC2020 enables distinction of agricultural tree crops with an overall accuracy higher than 85% for most tree crops, while the classification of European tree crops remains the most challenging. The classified tree crop class significantly improves the commission error rates in the main GEM-FnF2020 product (0.5–14.8%). Our proposed approach demonstrates strong potential for temporal transferability across the 2017–2025 period covered by AEF embeddings. This capability allows multi-year applications and change detection



based on models trained for a single year and represents a key next step in our research. Overall, the findings demonstrate that AEF embeddings combined with simple ML approaches support accurate, transferable, and computationally-efficient global forest mapping, with remaining limitations related to temporal resolution and feature interpretability. These results and the presented approach can support policy and regulatory decisions, including the EUDR, while the open-access release of the GEM-Forest datasets and trained models facilitates global use, further testing, and methodological development by the EO and forest monitoring communities.

1 Introduction

Forests, that cover around one-third of the Earth's land surface, are one of the most important ecosystems of the planet, as they play a crucial role in climate regulation, the global carbon cycle and biodiversity conservation (Cook-Patton et al., 2020; Hughes et al., 2021; Lewis et al., 2019; Raven et al., 2020; Smith et al., 2023). However, forests are subject to continuous change, influenced by both human activities and natural processes. These influences lead to both forest loss, resulting from factors such as deforestation, climate change and natural disturbances, and forest gain, achieved through effective forest management and restoration efforts (Bartels et al., 2016; Forzieri et al., 2022; Ma et al., 2023). Notably, from 2011 to 2020, forests acted as a net carbon sink, absorbing more carbon than they released, which is largely attributed to recent afforestation activities and improved forest management practices (FAO, 2022).

The advent of big data in Earth observation (EO) and cloud-based computational technologies enables near-real-time monitoring of status and dynamics of forests. With new policies, such as the European Union Deforestation Regulation (EUDR), the EU's new 90% greenhouse gas (GHG) emission reduction target (which includes the contribution of high-quality international carbon credits), the EU forest strategy for 2030 of the European Green Deal, and other national and regional policies, new challenges and opportunities arise in the era of big EO data.

Numerous national to global EO-based forest maps often serve as baseline layers in real-world applications, such as early-warning systems for deforestation monitoring and in policy- and decision-making on a national to global level. However, their accuracy and temporal availability vary across regions and climatic zones. Accurate and up-to-date forest cover information is essential for real-world applications. Recent years have been marked by attempts to monitor the state of global forests, especially aiming to support the EUDR. The EUDR aims to prevent the import of forest-related goods into the EU linked to deforestation or forest degradation after 31 December 2020 (Regulation (EU) 2023/1115). Therefore, recent and ongoing efforts are aimed to map the extent of global forests in 2020. Based on a recent 2025 review of 21 global forest/tree cover products, only two met the EUDR forest definition criteria. However, each evaluated dataset, including these two, failed to accurately distinguish between forests and other tree-based systems, e.g. agroforestry systems, generally resulting in overestimation of forest cover (Freitas Beyer et al., 2025). One of the two is the European Commission's Joint Research Center's Centre's (JRC) Global Forest Cover map for 2020 at 10m spatial resolution (GFC2020) (Bourgoin et al., 2026), which is specifically aimed to support the EUDR. GFC2020 was produced by combining multiple global forest-related, land cover, and ancillary datasets to map the maximum global forest extent for 2020. Its accuracy



65 highly depends on the quality of the input datasets, and its approach is limited in transferability to other years, as this would require up-to-date data for those years.

Many other global forest maps/products have been developed over the recent years. One of the most frequently used dataset is the Global Forest Change (GFC) dataset (Hansen et al., 2013) that informs about yearly forest losses and tree cover gain from 2000 onward, and is based on classification of multi-temporal Landsat data at a 30 m spatial resolution. However, this and other similar
70 global forest products could be described as a tree cover dataset, as it is often criticized for classifying tree crops as forest cover (Freitas Beyer et al., 2025; Tropek et al., 2014). For differentiating between forest and non-forest classes, general global land use / land cover datasets can also be utilized, such as the ESA World Cover product that shows superior performance compared to other 10m global land cover products with high accuracy for the forest class (Xu et al., 2024).

Some of the datasets aimed to map the extent of natural forests, nevertheless, the final forest class does not include planted forests,
75 such as the Natural Forests of the World 2020 by Neumann et al. (2025), or the planted forest category is merged with plantations used for agroforestry, e.g. in Global Forest Types dataset by Bourgoin et al. (2024 and 2025), or the layer is available only for 2015 at a limited 100 m spatial resolution in the Global forest management map by Lesiv et al. (2022). However, planted forests used for forestry purposes should be defined as forests based on the FAO and EUDR definitions. Other datasets successfully mapped the extent of both natural and planted forests, such as the Global Natural and Planted Forests dataset by Xiao et al. (2024).

80 Recent advances in Artificial Intelligence (AI), combined with the growing availability of large-scale EO data, have led to the emergence of EO foundation models and their derived embedding products. These models are trained on massive, heterogeneous EO archives to learn general-purpose representations of the Earth's surface, capturing spatial, spectral, and contextual patterns across biomes, sensors, and acquisition conditions. The introduction of EO embeddings represents a significant step in this direction, providing globally consistent, high-dimensional feature representations that are designed to be transferable across tasks, regions,
85 and time periods. Rather than optimizing for a single downstream application, embeddings aim to encode semantically meaningful information that can be reused across a wide range of EO analyses.

EO embeddings can be understood as ready-to-use feature representations that abstract raw satellite observations into a compact and information-rich space, enabling efficient application to downstream tasks such as clustering, classification, similarity search, and change detection. They can be provided both at pixel-level, such as in the case of Google DeepMind's Alpha Earth Foundation
90 (AEF) (Brown et al., 2025) and TESSERA (Feng et al., 2025), and at patch-level, as intermediate features of geospatial foundation models (e.g., TerraMind (Jakubik et al., 2025) and THOR (Forgaard et al., 2026)). This paradigm substantially lowers the barrier for large-scale EO analytics, as it allows simple and computationally efficient machine learning (ML) models to achieve competitive performance without extensive task-specific feature engineering or model tuning.

In the context of forest monitoring, such embeddings are particularly valuable, as they offer the potential to consistently distinguish
95 forests from structurally similar land-cover types, including tree crops, across diverse ecological and geographic settings. Recent studies have already demonstrated the practical utility of such embeddings for regional tree species monitoring in the United States (Gao et al., 2025) and in Italy (Ball et al., 2026), where EO embeddings outperformed composite-based multitemporal and



multimodal EO baselines. As a result, EO foundation model embeddings like AEF provide a promising starting point for scalable, multi-temporal, and globally transferable forest and land-cover mapping workflows.

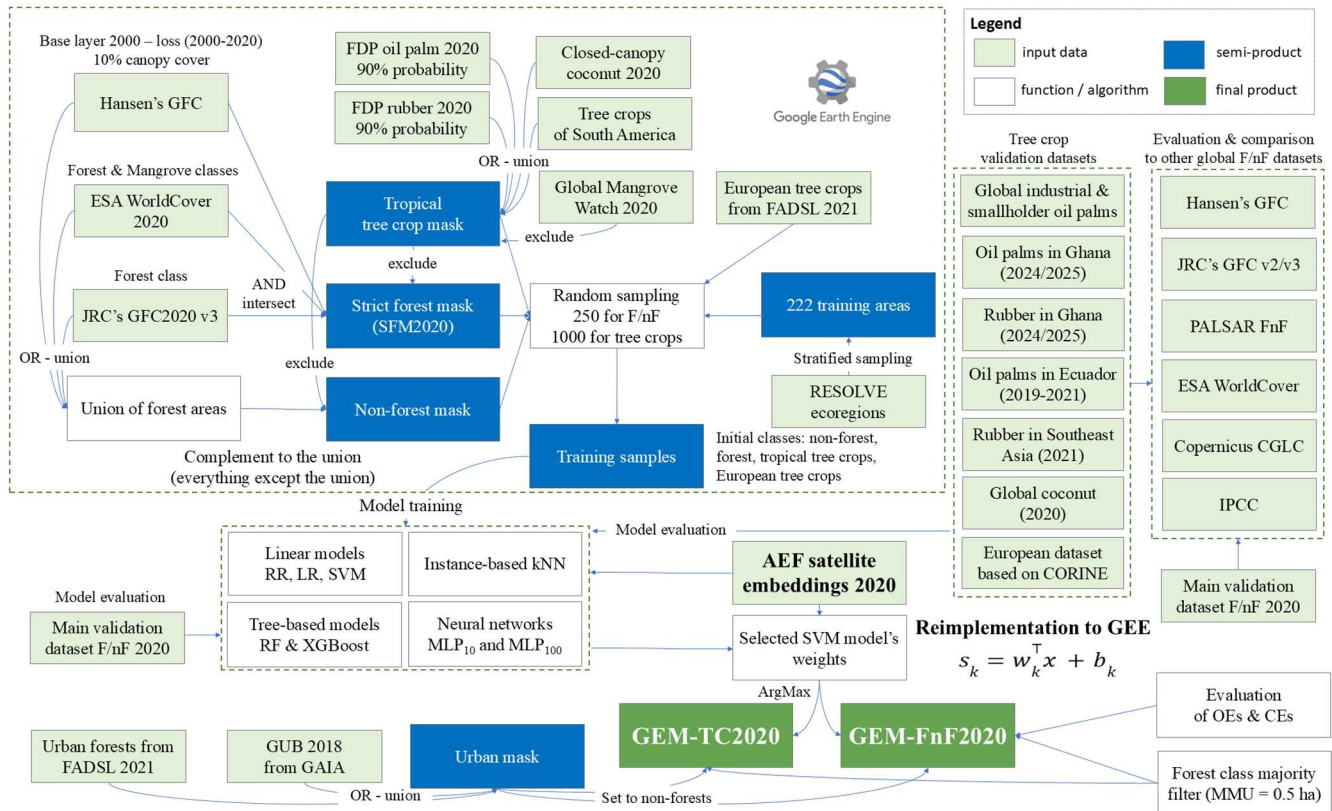
100 In this study, we introduce GEM-Forest, a global satellite embedding-based forest dataset in 10 m spatial resolution for 2020, and its associated products: GEM-FnF2020, a forest / non-forest (F/nF) classification, and GEM-TC2020, which further distinguishes non-forest areas containing tree crops. We introduce an effective automatic training data generation by intersecting multiple forest-related, land cover and plantation datasets to reduce uncertainty and limitations of individual input datasets. We investigate whether traditional ML methods can achieve competitive or superior performance in global F/nF classification compared to more complex
105 approaches, highlighting both the strengths and limitations of the embeddings and the classifiers themselves.

2 Data and methods

We used the AEF to develop a global F/nF classification at 10 m spatial resolution, with an additional tree crop class as a subclass of the non-forest class. Using AEF, we evaluated a set of lightweight supervised ML classifiers, including linear approaches (Logistic and Ridge Regression, linear Support Vector Machines - SVM), an instance-based approach (k-nearest neighbors - kNN)
110 and compared their performance with more advanced non-linear classifiers, such as Random Forests (RF), Extreme Gradient Boosting (XGBoost) and neural networks (Multi-layer Perceptron - MLP). Training data are generated through an automated training process across 230 training areas that proportionally represent all global biomes. We assessed the accuracy of the final 2020 F/nF maps through an independent set of ~21,000 global F/nF reference samples for the year 2020, supplemented by seven open-access regional and global validation datasets for tropical tree crop plantations and a developed validation dataset for European tree
115 crops. The GEM-Forest products (GEM-FnF2020 and GEM-TC2020) were produced by implementing model weights in GEE. By calculating the dot product between these weights and the AEF feature vectors, we identified the class with the highest probability for every global pixel. To meet the EUDR forest definition requirements, we mask out forests in urban areas and apply a majority filter to the forest class to mask out forest areas smaller than 0.5 ha. Each methodological step is detailed in the following paragraphs and visualised in Figure 1.

120 2.1 Forest definition

According to the FAO definition, forest is “Land spanning more than 0.5 hectares with trees higher than 5 meters and a canopy cover of more than 10 percent, or trees able to reach these thresholds in situ. It does not include land that is predominantly under agricultural or urban land use.” (FAO, 2023, p.7). The EUDR adopts this forest definition, while the "other wooded land" is excluded from its forest definition. To align with these definitions, we adopted these definitions, therefore we define forests as an area covered
125 by trees with at least 10% canopy cover, with at least 5 m in height and representing an area of at least 0.5 ha, that is not under agricultural or urban land use in 2020. The inclusion of areas covered by young trees that have not yet reached the height and canopy coverage thresholds, and temporarily unstocked areas or clear-cuts, where forests are expected to meet the physical parameters in the future, were omitted in this study.



130 **Figure 1. The full methodological pipeline used in this study.**

2.2 Input dataset - the Google DeepMind Alpha Earth Foundation's Satellite Embedding dataset

The main data source is the AEF's Satellite Embedding dataset, consisting of 64-dimensional feature vectors representing each 10 m pixel's multi-modal, multi-temporal EO signal over a calendar year, with the current coverage from 2017 to 2025. These embeddings
 135 are produced by a deep geospatial representation learning model that fuses inputs from Landsat, Sentinel-2, and Sentinel-1 data, enhanced with temporal and spatial features (Brown et al., 2025). During training, the model learns to reconstruct target variables from other radar (from ALOS PALSAR-2), LiDAR (GEDI mission), environmental (topographic data from Copernicus DEM, meteorological data from ERA5-Land, gravity field information from GRACE), and annotated geolocated datasets (from Wikipedia and the Global Biodiversity Information Facility).

140 2.3 Preparing 'strict' forest, non-forest, tree crop and urban masks

In the first step, we prepare a strict forest mask for which we intersect three globally available forest-related and land cover datasets: 1) the ESA WorldCover's (WorldCover) Forest and Mangrove classes in 10 m spatial resolution 2) JRC's Global Forest Cover for 2020 (GFC2020) version 3 in 10 m spatial resolution and 3) the Hansen et al.'s GFC dataset in 30 m spatial resolution, with a



145 minimum canopy cover threshold of 10%, where the forest loss layers from 2000 to 2020 were used to exclude non-forest areas from the base-layer from 2000. The intersection of these three datasets represent our ‘strict’ forest mask for 2020 (SFM2020) and serves as a baseline for the subsequent training data generation.

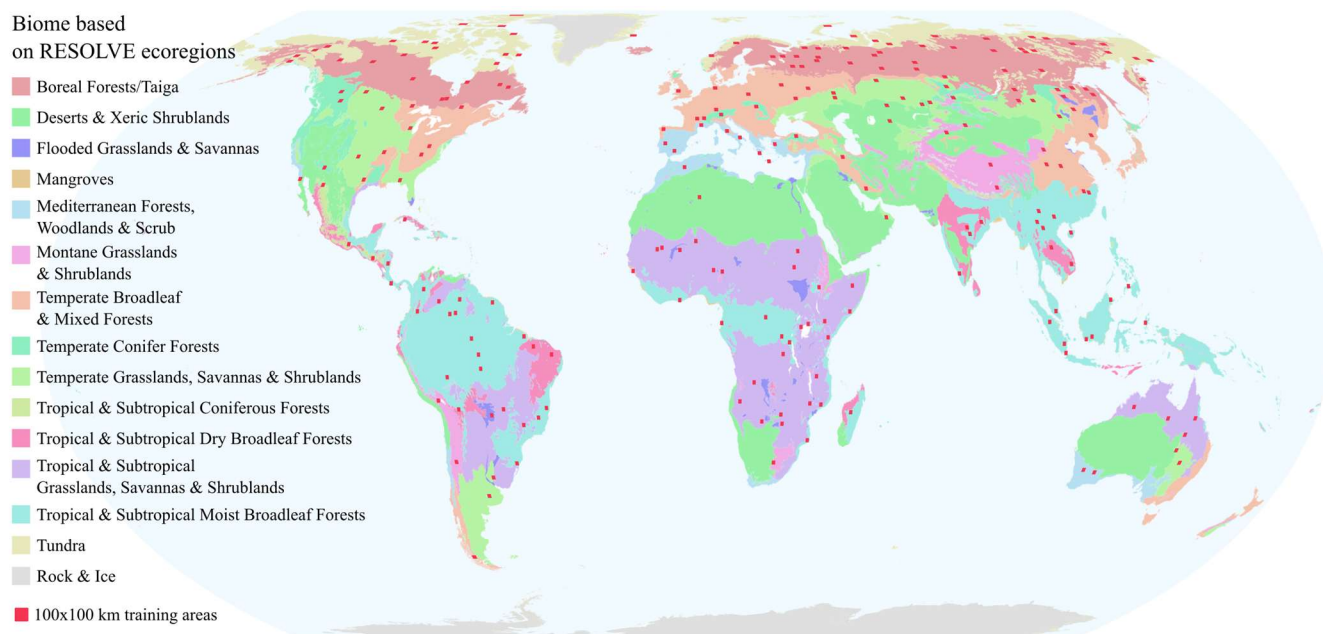
To generate a tree crop mask, we used a union of global and semi-global maps of tree crops, specifically, 1) the 10m commodity probability layers for palm and rubber plantations from the Forest Data Partnership (FDP) (Forest Data Partnership, 2025), specifically pixels that had higher than 90% probabilities of occurrence for the year 2020; 2) the 20 m global map of closed-canopy coconut palm (Descals, 2023; Descals et al., 2023), 3) a 10 m dataset for tree crops in the EU, i.e. trees predominantly used for agricultural practices (olive trees, fruit trees, nut trees) from the 2021 Forest Additional Support Layer (FADSL) from the High Resolution Layer Tree Cover and Forests product of the Copernicus Land Monitoring Service (CLMS) (European Environment Agency, 2024) and 4) the 10 m tree crop map of South America, version 2 from Jiang et al. (2026), specifically pixels that had higher than 90% probabilities of occurrence for the year 2020. We have moreover used the Global Mangrove Watch data (Bunting et al., 2022b, a) to mask out (exclude) mangrove areas from the tree crop mask. Pixels corresponding to the tree crop mask were subsequently excluded from the SFM2020.

The non-forest mask is defined as the complement to the union of all used forest layers, that means everything except the union of three used forest layers (GFC2020, GFC and WorldCover). Pixels corresponding to the tree crop mask were masked out (excluded) from the non-forest mask.

160 To align with the forest definition regarding the exclusion of urban forests, we created an urban mask by combining the globally available Global Urban Boundaries for 2018 (GUB) from the global artificial impervious area (GAIA) data (Li et al., 2020) with urban forest layers from the FADSL (European Environment Agency, 2024) for the year 2021, which is available only for the EU. This urban mask was used in the post-classification step to remove urban areas and urban forests from the final classification, and these areas were reassigned to the non-forest class.

165 **2.4 Training data preparation and ML model training in all biomes**

To train a ML model, we first randomly generated 100x100 km areas across the globe, whose distributions were proportional to the extents of 14 biomes of the world based on the RESOLVE ecoregions (Dinerstein et al., 2017). This step included a generation of random points using a stratified sampling scheme within each biome with a subsequent application of a 100x100 km square buffer, while the overlapping areas were subsequently excluded from the final selection. Due to the random sampling approach, some areas became under-represented, especially areas with tree crops. Therefore, we added 21 representative 100x100 km areas representing large-scale palm, rubber and coconut plantations, and 13 areas representing European tree crops. This step reinforced the inclusion of tree crop areas in training data generation. In the end, a total of 230 training locations with a square 100x100 km area were selected.



175 **Figure 2. Distribution of 100x100 km locations for training (red squares) over the world's biomes based on the RESOLVE ecoregions layer. Map projection: Equal Earth (EPSG: 8857)**

180 Within these selected training locations, we generated random points based on the forest, non-forest and tree crop masks. The tree crop mask was divided into two masks: the tropical and the European tree crop masks. Based on the initial tests, further subcategorization of the crop mask did not yield better results qualitatively nor quantitatively. In each training location, 250 random points were generated for forest and non-forest classes, and 1000 points for the tree crops classes, each with a 10x10 m square buffer. Only points whose 10x10 m buffered area was entirely (100%) within a single land-cover class (forest, non-forest or tree crops) were retained for training to ensure the selection of highly representative training samples. In total, we obtained 47,308 training points globally (~14,500 forest, ~28,300 non-forest training and ~3,300 tropical and ~1,100 European tree crop points) that we used to train our ML models, specifically Logistic and Ridge Regression (LR and RR), linear Support Vector Machines (SVM), kNN, RF, XGBoost and neural networks, represented by MLPs with 10 and 100 neurons (MLP₁₀ and MLP₁₀₀). We used the default hyperparameters for each ML model, based on the scikit-learn version 1.6.1 (scikit-learn.org, (Pedregosa et al., 2011) and the XGBoost version 3.2.0 (xgboost.readthedocs.io/en/release_3.2.0, (Chen and Guestrin, 2016) Python libraries. Building upon the workflow for automated training sample generation based on a strict forest mask previously implemented by Onáčillová et al. (2023) for Europe, this study adapts and scales the logic for global application using globally available datasets.

190 In the initial stage, we classified forest, non-forest, and tropical and European tree crops, while the final datasets include two versions: 1) dataset representing the 2020 F/nF map where the tree crop classes are merged into the non-forest class (GEM-FnF2020) and 2) the dataset representing forest, non-forest and tree-crops for 2020, where the tropical and European tree crops are merged into one tree crop class (GEM-TC2020). Urban forests were masked out from both products based on the urban mask, and a 0.5 ha



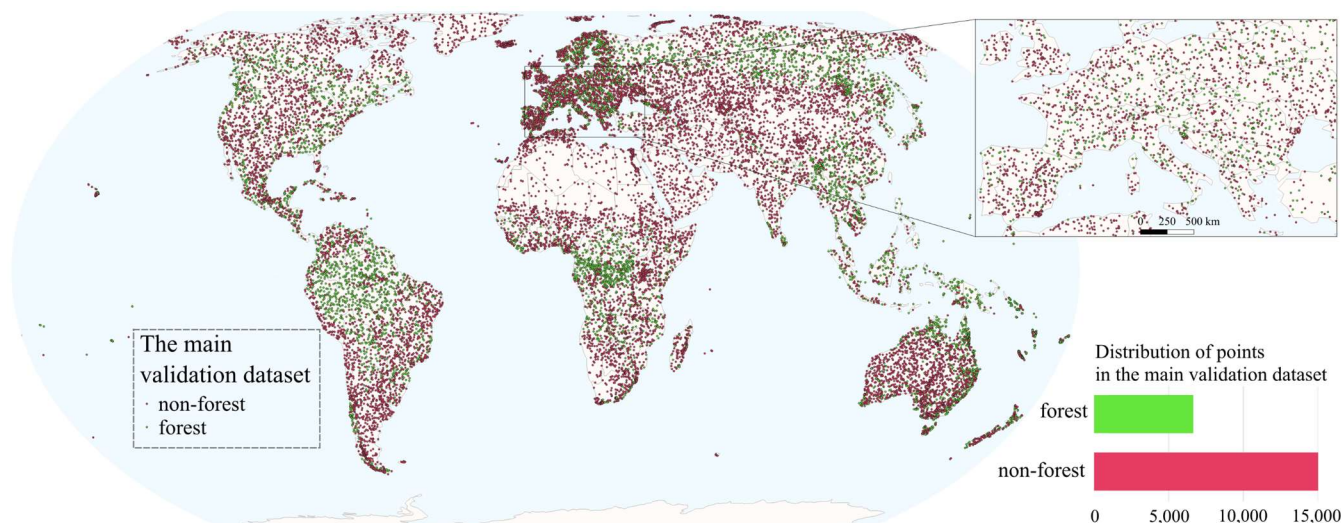
195 majority filter was applied to the forest class to align with the FAO and EUDR forest definitions. We compared the achieved results with an alternative setting for F/nF classification trained solely on forest and non-forest training samples (on 42,843 samples), in order to assess the potential of using only these two classes and to evaluate the added value of explicitly including tree crop classes in the training process (as in the GEM-FnF2020 map).

2.5 Accuracy assessment

200 To statistically evaluate the results, we calculated the overall accuracy (OA), class-specific, macro F-score (overall average) and weighted F-score, omission and commission errors (OE and CE) for the GEM-FnF2020 dataset. OE and CE were calculated to assess the effect of forest areas omitted from the classification and areas that were classified as forests, but were not covered by forests in reality. The tree crop class of the GEM-TC2020 map was assessed though OA, while commission errors corresponding to forest and non-forest classes were also evaluated. The validation datasets used for these purposes are described in detail in the
205 following subsections. It should be noted that the accuracy assessments for GEM-FnF2020 and GEM-TC2020 were conducted without applying a 0.5 ha majority filter to the forest class.

2.5.1 Accuracy assessment of the GEM-FnF2020 map

To validate the accuracy of our GEM-FnF2020 map, we used the *Validation dataset for the global map of forest cover 2020, v.2* from JRC (Colditz et al., 2025) that was used to validate the GFC2020 product (Bourgoin et al., 2026), further referred to as the
210 *main validation dataset*. The main validation dataset included more than 21 thousand samples covering the entire land area of the globe, except Antarctica. The categorical distribution of forest and non-forest area was 35% and 65% (~6,000 and ~15,000 areas), respectively, which represents the actual forest cover share over land globally. To replicate the validation process used in Bourgoin et al. (2026), we excluded points from the original dataset that had not assigned ground truth values strata information or were not overlapping with the FAO Global Administrative Unit Layer dataset (FAO, 2015), resulting in a total of 21,612 validation points.
215 Based on an initial quality assessment using our urban mask and time series evaluation of high-resolution (HR) imagery from Google Earth, we identified 21 points in the main validation dataset that corresponded to urban forest areas but were labeled as forest. The ground truth labels of these points were subsequently changed to non-forest (class 0).



220 **Figure 3. Spatial and statistical distribution of F/nF points in the main validation dataset, and a zoomed-in view of Europe as the region with the highest point density. Map projection: Equal Earth (EPSG: 8857)**

2.5.2 Evaluation of misclassified areas in the GEM-FnF2020 map

To evaluate misclassified areas in the GEM-FnF2020 map, we derived a random subset of 433 points from the main validation dataset that represented OEs and CEs for the forest class. These OEs and CEs were independently visually interpreted for the presence or absence of forest cover for 2020 based on high-resolution time series imagery in Google Earth Pro (GEP). For ambiguous cases, we performed a visual interpretation using the SAR & Optical Time Series based on radar Sentinel-1 and multispectral Sentinel-2 data that enables the assessment of vegetation seasonality and temporal stability over a longer timeframe (since 2017 with both satellites) with high temporal resolution. This dataset thus allowed a two-way accuracy assessment and a quality check between the results of our classification (GEM-FnF2020) and the main validation dataset.

230 In addition to standard accuracy metrics, all points were subjected to qualitative error attribution based on visual inspection and time-series analysis, with mismatches grouped into thematic categories such as sparse or scattered woody vegetation, forest edge or transition zones, shrub-tree confusion, land-use versus land-cover inconsistencies, riparian or wetland complexity, urban vegetation, and fragmentation effects. This error evaluation approach was used to explore and understand 1) true classification errors, 2) definition-driven mismatches related to forest structure and spatial continuity across different ecological and land-use contexts 3) 235 and incorrectly assigned labels in the main validation dataset. This validation dataset is referred to as the error validation dataset.



2.5.3 Validation of the tropical tree crop class of the GEM-TC2020 map

For the validation of the tree crop class of the GEM-TC2020 map in the tropics, we used global and regional open-source validation datasets for tropical plantations of oil palm, rubber, coconut and other palm species.

- For validation of oil palm plantations, we used three datasets: 1) 1,374 of globally distributed industrial oil palms for 2021 and 2) 531 globally distributed smallholder oil palms, both based on Descals (2024a) and Descals et al. (2024) *v1.2*, and 3) 164 points (dense and organized plantations, suggesting industrial oil palms) that were unchanged between 2019 and 2021 from Ecuador (Fundación EcoCiencia, 2025) *v1.0*.
- Rubber was validated using 217 monoculture rubber points in South-East Asia for 2021 (Descals, 2024b; Sheil et al., 2025) *v1.1*.
- Coconut areas were validated using 327 globally distributed points of dense open-canopy and closed-canopy coconut palm plantations for 2020 (Descals, 2023; Descals et al., 2023). These datasets were extended by palm species that are not coconut palm for 2020 from Descals (2023) and Descals et al. (2023).

2.5.4 Validation of European tree crops of the GEM-TC2020 map

For the validation of the tree crop class of the GEM-TC2020 map in Europe, we created a validation dataset based on the CORINE Land Cover 2018 (European Environment Agency, 2020) to identify stable tree crop areas across Europe. CORINE areas classified as olive plantations (class 223) and fruit tree and berry plantations (class 222) above a minimum area threshold of 25 ha were selected, with representative points generated either as centroids or as size-proportional random samples for very large polygons (for more details see the Appendix A). These selected points were further validated using a time series of high resolution imagery in GEP to ensure the presence of tree crops around the reference year 2020. The final dataset included 303 points for validation.

2.6 Comparison to other global F/nF and tree cover datasets

To compare the final GEM-FnF2020 map with other globally available F/nF and tree cover datasets, we compared our dataset to the following seven global datasets, detailed in Table 1: 1) GFC with a base layer from 2020, but with excluded areas deforested between 2000 and 2020 (Hansen et al., 2013), 2) the Global 4-class PALSAR-2/PALSAR Forest/Non-Forest Map (PALSAR FnF) for 2020 (Shimada et al., 2014), 3) Copernicus Global Land Cover Layers (CGLCL) for 2019 (Copernicus Land Monitoring Service, 2015), 4) Global 2020 Forest Classification for Intergovernmental Panel on Climate Change Aboveground Biomass Tier 1 Estimates (hereafter referred to as IPCC) (Hunka et al., 2024a, b), 5) ESA WorldCover for 2020 (Zanaga et al., 2022), 6) GFC2020 v2 and 7) GFC2020 v3 (Bourgoin et al., 2026).

265 **Table 1. Characteristics of global datasets used in the comparison**

Dataset name, version	Year	Spatial resolution	FAO forest definition	Citation
GFC, v1.12	2000	30 m	no	(Hansen et al., 2013)
PALSAR FnF, v2.0.0	2020	25 m	yes	(Shimada et al., 2014)
CGLCL, v3	2019	100 m	no	(Copernicus Land Monitoring Service, 2015)
IPCC, v1	2020	30 m	yes	(Hunka et al., 2024a, b)
WorldCover, v100	2020	10 m	no	(Zanaga et al., 2022)
GFC2020, v2 & v3	2020	10 m	yes	(Bourgoin et al., 2026)

2.7 Computational effectiveness of data preparation, validation and data export process

To ensure computational efficiency and feasibility of the data preparation workflow, including the generation of forest, non-forest, and plantation masks; the preparation of training locations; the creation of training datasets; and the extraction of features from the AEF for both training and validation points, we used the Google Earth Engine (GEE) platform (Gorelick et al., 2017), which hosts most required datasets described in the previous sections as well as the AEF. Some datasets were needed to be ingested to GEE.

270 Subsequently, ML model training and validation were conducted in a local Python environment. As a final step, the learned weights and biases of the linear models were re-implemented within a GEE processing pipeline applied to the AEF to generate the final GEM-FnF2020 and GEM-TC2020 maps. These products were exported from GEE and archived in a publicly accessible repository in Zenodo. For data export, the study area was tiled into $5^\circ \times 5^\circ$ spatial grids that enabled an efficient export of results at 10 m spatial resolution.

2.8 Model inference using linear models

An important advantage of linear models, particularly RR and SVM, is their straightforward integration into the proposed processing pipeline for large-scale F/nF and tree crop mapping, e.g. in GEE. In these cases, only the classifier weight vectors and intercepts for each class are required that allows the models to be implemented as simple linear equations applied to the embedding feature vectors. For each pixel, the class score s is computed as the dot product of the embedding feature vector x with the classifier weight vector w_k , plus the intercept b_k :

280

$$s_k = w_k^\top x + b_k, \quad (1)$$

Class decision scores are computed for each pixel, and the final class is assigned by selecting the class with the highest value, consistent with the One-vs-Rest (OvR) formulation used during training. This approach allows efficient large-scale deployment, since the models require minimal computation at inference.

285



3. Results and discussion: technical validation

3.1 Summary of validation results for the GEM-FnF2020 map

To assess the generalization capacity and discriminative power of the AEF satellite embeddings on previously unseen data, we evaluated a range of traditional ML classifiers on an independent global validation dataset, on the main validation dataset. The embeddings were used directly as input features, without task-specific fine-tuning, allowing the evaluation to isolate the representational quality of the AEF feature space.

Our final GEM-FnF2020 map is produced by merging the tropical and European tree crop classes with the non-forest class, which achieved high accuracies both on the main F/nF validation dataset and on the selected tree crop validation datasets. Across all evaluated models, OAs consistently achieved 91–92%, with macro F1-scores between 0.89 and 0.91, overall OEs and CEs of 9.60–11.77% and 9.26–10.33%, respectively (Table 2). This stable performance across fundamentally different classifiers indicates that the AEF embeddings encode a highly informative and task-relevant structure for global F/nF discrimination. At the same time, the dataset remains challenging for certain region- and tree crop-specific classes and provides a meaningful benchmark for evaluating the limits of current EO embeddings, as summarized in the following section 3.2.

Table 2. Overall and class-based accuracy and error metrics for the tested algorithms. Bolded results represent the best achieved accuracies, while SVM (underscored) was selected for further evaluation.

Model	OA	macro-F1*100	w-F1 *100	overall OE	overall CE	OE F	CE F	OE nF	CE nF
kNN	90.65	88.84	90.60	11.56	10.72	17.21	14.04	5.91	7.40
LR	91.77	90.20	91.74	10.13	9.45	14.99	12.43	5.27	6.47
RR	91.07	89.18	90.95	11.77	9.67	19.00	11.34	4.53	8.00
<u>SVM</u>	<u>91.60</u>	<u>89.99</u>	<u>91.56</u>	<u>10.34</u>	<u>9.66</u>	<u>15.28</u>	<u>12.73</u>	<u>5.40</u>	<u>6.59</u>
RF	90.95	89.04	90.83	11.89	9.83	19.16	11.58	4.63	8.07
XGBoost	91.54	89.89	91.49	10.54	9.63	15.87	12.43	5.22	6.82
MLP ₁₀	92.05	90.56	92.03	9.60	9.26	13.82	12.53	5.39	6.00
MLP ₁₀₀	91.62	90.04	91.59	10.22	9.69	14.93	12.93	5.52	6.46

Note: w-F1 = weighted F1-score, F = forest, nF = non-forest. F1-scores were multiplied with 100 for better readability.

The comparison with the F/nF classification trained without tree crop data showed comparable on the main validation dataset. Although the overall and class-specific accuracies were promising, and in most cases better (OA of 91–92%, macro F1-score of 0.90–0.91, with slightly lower forest OEs and higher forest CEs compared to GEM-FnF2020; see Appendix B), subsequent qualitative assessment in regions dominated by tropical plantations, together with statistical evaluation using tree crop validation datasets, revealed clear limitations, with forest CEs higher than 70% in most cases (Appendix C). Specifically, training the models



310 exclusively on forest and non-forest samples did not provide sufficient information to reliably classify tree crops as non-forest areas. These results highlight the limitations of using a global F/nF validation dataset alone, particularly for assessing product performance in identifying tree crop areas as non-forest. Even with ~21,000 validation points, the distribution of non-forest areas representing tree crops may be sparse, causing their misclassification to have minimal impact on overall metrics. For this reason, we employed additional tree crop validation datasets and included tree crop training data, classifying the tree crop subclass separately in the initial
315 GEM-FnF2020 classification, which was subsequently merged with the non-forest class.

3.2 Summary of validation results for the tree crop class of the GEM-TC2020 map

The evaluation of the tree crop class in the GEM-TC2020 map using regionally or globally available tree crop validation datasets shows variability across crop types and geographic contexts. The highest accuracies were achieved for the global industrial and smallholder oil palm validation dataset (OA: 87–96%; forest commission errors - forest CEs: below 7%), with generally slightly
320 higher OAs and lower forest CEs for industrial oil palms in most models (Figure 4 and Figure 5). This reflects that the large, homogeneous, closed-canopy structure of industrial plantations is easier to differentiate from forests using the AEF embedding space. Oil palms in Ecuador exhibited slightly lower OAs and higher forest CEs, which we attribute to reduced separability of semi-wild plantations, greater landscape heterogeneity, smaller plantation sizes and mixed management systems. These factors reduce the distinguishability of oil palms and tree crops in general from forests in the AEF feature space. Notably, smallholder oil palms
325 also achieved very high accuracies in this evaluation, indicating that the method effectively captures both plantation types. These results are consistent with findings using EO data, specifically Sentinel-1 and Landsat time series, in Descals et al. (2024), who reported 91% class-specific producer's accuracy for industrial oil palms and 71% for smallholders, although in our study smallholder oil palms were classified comparably good compared to industrial plantations. Using the same oil palm validation dataset, Clinton et al. (2024) reported a producer's accuracy of 82% for their global palm community model for 2020 at a palm probability threshold
330 of 0.82. It should be noted that the comparison of our achieved OA only on positive samples (points classified as palm), is not directly comparable to their overall producer's accuracy reported on both palm and non-palm samples.

Similarly, high OAs and low forest CEs were also achieved by rubber points in Southeast Asia (OA of 84–94% and forest CEs 5–11%, except for RF and RR models). Based on the rubber validation dataset used in Southeast Asia, the reported producer's accuracy for Wang et al. 's map (Wang et al., 2023) of rubber monoculture distribution showed substantially lower accuracy of $68.1 \pm 3.9\%$,
335 based on the validation in Sheil et al. (2025).

Coconut plantations show relatively high accuracies (OA of 73–93%), but higher forest CEs (6–19%) depending on canopy closure, with closed-canopy coconuts outperforming open-canopy coconuts, consistent with results from the global coconut plantation layer (Descals et al., 2023). This highlights the importance of structural density in distinguishing forests from tree crops. Moderate accuracies with the highest forest CEs were achieved by the other palms dataset.

340 Even for the European tree crop validation dataset, where moderate OAs were achieved (66–45%, depending on the ML model), the proportion of forest CEs remains low, i.e., 10–16%. Consequently, a larger share of misclassifications occurred as non-forest (non-forest CEs). This is not problematic when the primary objective is F/nF separation, as the GEM-FnF2020 map correctly



classifies these areas as non-forest. Lower OAs for European tree crops are likely due to limited training data, as only 1,133 European tree crop points were used to train the models. Lower OAs may also reflect the fragmented parcel structure and mixed agricultural mosaics typical for European landscapes.

345

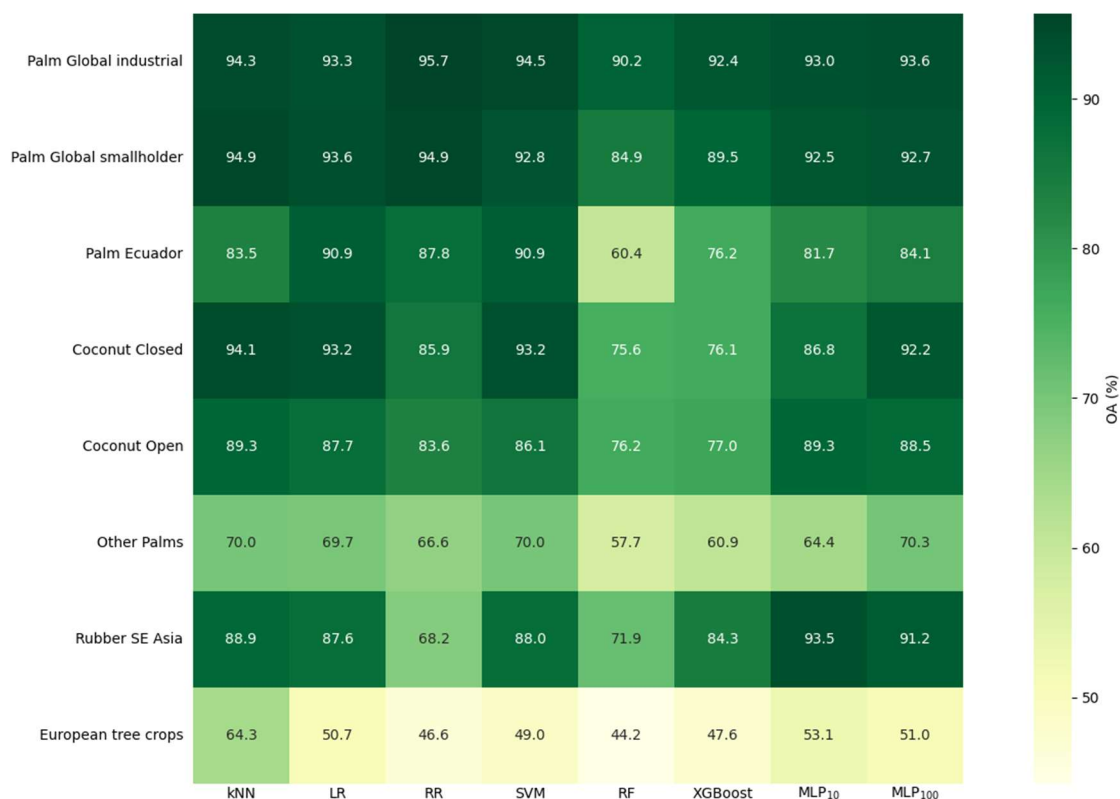


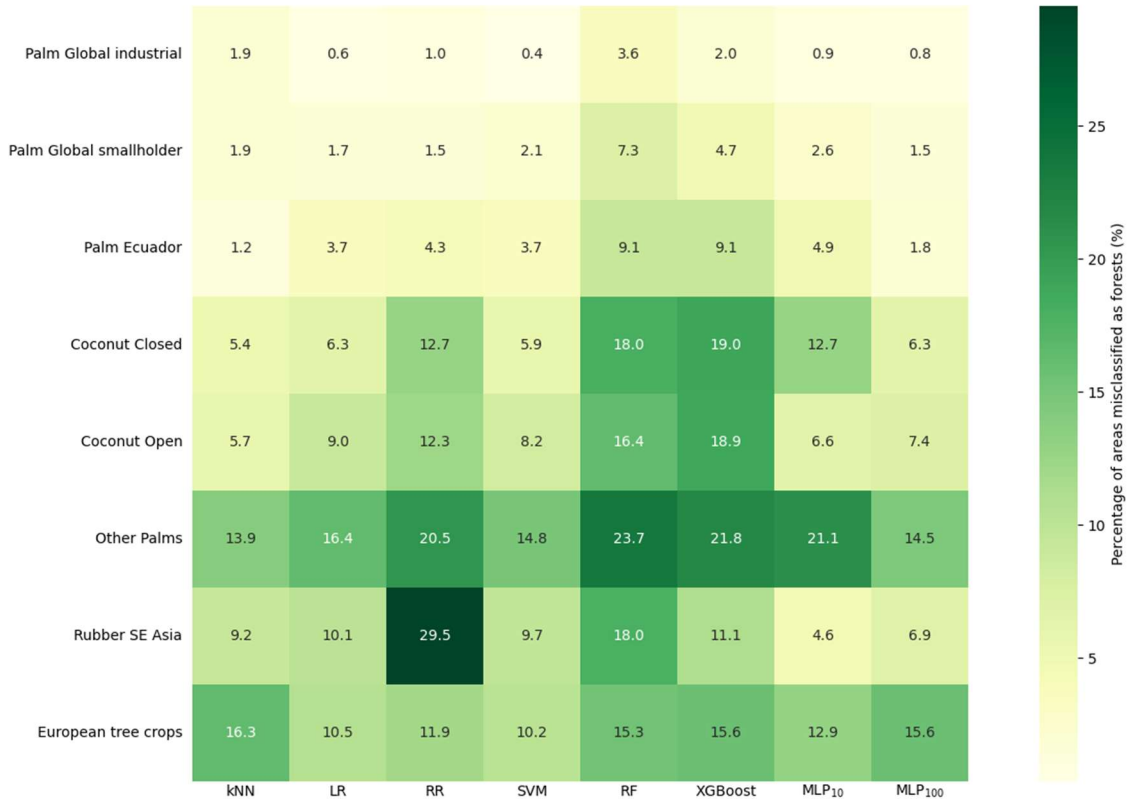
Figure 4. Overall accuracy of used tree crop validation datasets on the GEM-TC2020 map.

Overall, these results show that the GEM-TC2020 map can effectively separate tree crops from forests across diverse contexts, with performance determined by plantation size, canopy structure, landscape heterogeneity, and training data availability, highlighting both the strengths and limitations of the AEF-based classification approach for global tree crop mapping.

350

Across models, the highest average performance (considering OA and CEs, i.e., tree crops incorrectly classified as forest in the GEM-TC2020 map) was achieved by kNN, followed by the linear models (RR, LR and SVM) and neural network approaches (MLP), whereas tree-based ensembles (RF and XGBoost) performed worst (Figure 4, Figure 5 and Appendix B). These results support the assumption that the use of more complex nonlinear models does not necessarily improve classification performance in this case and may even underperform compared to linear or instance-based approaches. It further suggests that the AEF embedding space already provides a well-structured representation in which class separability can be effectively exploited by relatively simple models.

355



360 **Figure 5. percentage of areas misclassified as forest class in the GEM-TC2020 map based on the tree crop validation datasets.**

3.3 Detailed performance evaluation of ML models for GEM-FnF2020 and GEM-TC2020 maps

3.3.1 Instance-based interpretation: k-nearest neighbors

The kNN classifier achieved an OA of 90.65% and a macro F1-score of 0.89 on the primary validation dataset. It demonstrated superior performance in tree crop validation, where it yielded the highest OA and lowest forest CE rates. Furthermore, the kNN model outperformed all others in F/nF classification when tree crops were reclassified as non-forest (Appendix D). Moreover, kNN showed best performance on 4 out of 9 tree crop validation datasets, specifically for both coconut, smallholder oil palms and European tree crops, while for coconut plantations showed the lowest misclassifications as forests. As an instance-based learner that relies solely on local neighborhood similarity, its strong performance provides direct evidence that the AEF embeddings cluster semantically similar land-cover types in the 64-dimensional feature space. In contrast, European tree crops exhibited the highest misclassification rate for kNN, with 16.3% of samples incorrectly identified as forest.

The combination of strong overall performance and confusion mainly between forests and specific tree crops indicates that the representations separate most land-cover types well, while classes with similar vegetation structure remain less distinct. This likely reflects overlap between natural forests and certain perennial crops in the embedding feature space. Because kNN does not learn



375 feature transformations or class-specific decision boundaries, these results provide a conservative estimate of the separability achieved by the AEF embeddings.

3.3.2 Linear models: logistic regression, ridge regression and linear SVM

LR, RR, and Linear SVM achieved very similar performance, with overall accuracies of 91.07–91.77% and macro-averaged F1-scores of 0.89–0.90. Among them, LR generally ranked among the top performers in overall and class-specific results for F/nF
380 separability (Table 2). RR achieved the highest overall accuracy for the industrial palm oil validation dataset, but performed worst for rubber in SE Asia. The strong performance of linear classifiers indicates that forest-relevant information is already well aligned with simple linear decision boundaries that require only minimal model complexity to extract. Remaining errors appear to result from similarities in the embedding representations rather than limitations of the models themselves.

We selected the linear SVM to produce the final GEM-FnF2020 and GEM-TC2020 maps. This model provided high accuracy for
385 the forest class, with balanced OE (15.3%) and CE (12.7%). Furthermore, it maintained consistently strong performance across all tested tree crops, with a mean OA of 78% and a low average misclassification rate as forest (7%). Beyond its predictive performance, the linear SVM offered a significant technical advantage due to its linear formulation. This structure permitted a straightforward implementation of the model weights via Eq. 1. Consequently, we calculated class decision boundary scores directly within GEE, which ensured computational efficiency for global applications.

390 3.3.3 Non-linear models: RF, MLP and XGBoost

Non-linear models such as MLP₁₀₀, MLP₁₀, RF and XGBoost achieved competitive OAs (90.95–92.05%) and macro F1-scores (89.04–90.56), comparable to linear models. The overall best results on F/nF separation was achieved by single-layered MLP with 10 neurons (Table 2). Despite their greater expressive capacity, none of the non-linear models provided substantial improvements over linear approaches or kNN. MLP₁₀ only marginally outperformed individual linear models, compared to SVM for OA (0.45%
395 difference) and for macro F1-score (0.0057 difference).

A detailed analysis of tree crop class-based performance showed instability between different tree crops. RF and XGBoost showed the lowest average OA for tree crop classifications with the highest forest CE rates (Appendix D). In contrast to the Linear SVM, which provided consistent results across all tree crops, the non-linear models exhibited lower accuracies and higher forest misclassification rates for specific tree crop classes. Notably, despite having the highest aggregate OA for F/nF classification, the
400 MLP₁₀ underperformed compared to the SVM in five out of eight tree crop validation datasets. Similarly, tree-based models like RF and XGBoost showed a distinct OA drop-off for oil palms in Ecuador and for other palms, with accuracies between 58% and 76%. non-linear models also often achieved the highest forest CE rates, with up to 24% for other palms using RF. This strengthens that the dominant discriminative structure in the AEF embedding space is effectively captured by relatively simple / linear decision surfaces. Increasing model complexity fails to resolve underlying class overlaps; instead, it tends to degrade generalization through
405 overfitting, as evidenced by the inconsistent performance of non-linear models across different tree crop classes.



3.4 Feature space structure analysis of the validation datasets

The t-SNE, directly performed on the AEF embedding of each data point, visualization of the validation feature space provides complementary qualitative insight (Figure 6). The dominant non-forest class forms a dense and well-separated cluster, explaining the consistently high OAs. In contrast, forests and tree crops exhibit substantial overlap, consistent with the observed misclassification patterns across all classifiers. These errors therefore reflect genuine semantic similarity in the embedding space rather than overfitting or model failure.

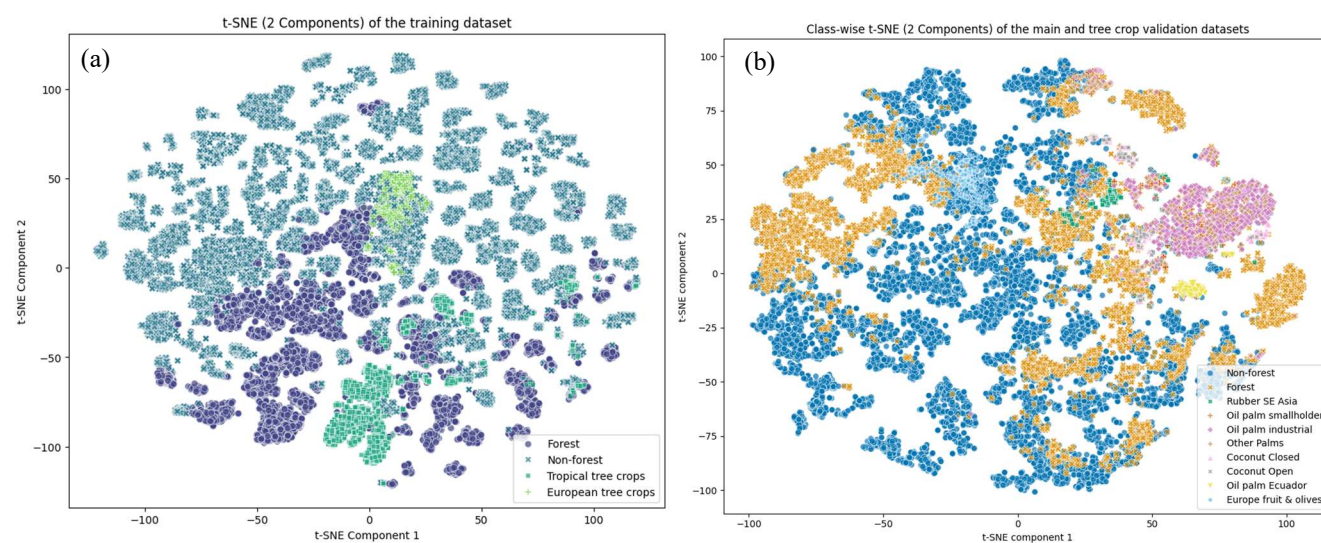


Figure 6. Separability of the training dataset (a) and validation datasets (b), including both the main validation dataset and class-wise tree crop validation datasets, through the two-dimensional feature space of the t-SNE plot.

3.5 Exploration of identified omission and commission errors

The error validation dataset, that helped to explore the primary sources of disagreement, consisted of 241 forest and 192 non-forest points according to the main validation dataset, representing 230 OEs and 203 CEs. Based on 433 randomly selected error samples, the dominant source of disagreement (62%) in the final GEM-FnF2020 map was related to areas with sparse or scattered woody vegetation and shrub-tree confusion. These cases likely reflect the inherent difficulty of differentiating transitional vegetation types within the AEF embedding representation.

Approximately 27% of the disagreements were associated with forest edges and transition zones, which may represent problematic assignments due to the 10 m spatial resolution of the input AEF embedding dataset in combination with differences in interpretation scale. While the GEM-FnF2020 map applied a minimum mapping unit (MMU) of 0.5 ha, the reference labeling procedure in the main validation dataset in some cases also considered the surrounding 100x100 m context that could potentially contribute to mismatches between map predictions and reference labels.



The remaining disagreement cases (11%) were linked to land use versus land cover inconsistencies, particularly trees located within agricultural land use that were classified as forest (6%), indicating a limited but expected confusion between tree crops and forest areas. Additional sources of land use/land cover confusion included forested patches within urban environments (3%), that reflect potential limitations of the applied urban mask in excluding tree-covered urban areas. Locations affected by riparian or wetland complexity represented 2% and likely reflect the structural heterogeneity and transitional nature of riparian and wetland ecosystems, which complicate F/nF discrimination at the spatial resolution and MMU of the AEF input data.

A potential source of disagreement arises from the forest definition used in the main validation dataset, which includes areas where trees are temporarily below the minimum height threshold of 5 m (e.g., in a regeneration or regrowth phase) or where the land is currently unstocked but intended for forest use in the future. This aspect of the definition was not applied in our GEM-FnF2020 product, as it cannot be directly observed from EO data, which form the basis for the AEF embeddings. In such areas, trees may not yet reach the physical definitional thresholds in situ in 2020 (5 m height, $\geq 10\%$ canopy cover, and a MMU of 0.5 ha), potentially resulting in OEs when comparing mapped forest in our GEM-FnF2020 product to reference labels in the main validation dataset.

Distinct regional clusters of disagreement further illustrate the interaction between forest definition and ecological context. In boreal regions of northern Europe and North America, discrepancies were concentrated in sparse and open forest formations and forest-tundra transition zones, where low canopy density challenges the delineation of continuous forest cover. In tropical and subtropical regions, particularly in savanna-dominated landscapes of Africa and northern Australia, disagreements were frequently associated with open woodlands and shrub-tree mosaics, where scattered trees generate forest-like spectral signatures without meeting canopy continuity requirements. In intensively managed agricultural regions, especially in Europe, misclassifications were dominated by riparian vegetation, shelterbelts, and small fragmented patches, emphasizing the influence of minimum width and area thresholds embedded in the FAO/EUDR forest definition.

It should be noted that when comparing the labels from the main validation dataset with our interpretation, only 101 points showed clear agreement between the two (71 forest and 30 non-forest). A substantial proportion of points (209) were located in areas with sparse or scattered woody vegetation, where shrub-tree confusion and transitional land-cover characteristics made assignment to forest or non-forest categories uncertain, even when using high-resolution imagery in GEP and radar and optical time series analysis, without in situ information on vegetation height or canopy density. The remaining 123 points showed discrepancies between the two interpretations, corresponding to potential commission- and omission-type differences. This indicates that these 123 points, that represents 28% of the identified OEs and CEs, may in fact reflect correctly classified F/nF areas in our GEM-FnF2020 map, suggesting that the actual accuracy of the product could be higher than indicated by comparisons with the main validation dataset alone. Therefore, the use of local or regional F/nF validation datasets is recommended to further assess accuracy and identify the underlying causes of errors in the GEM-FnF2020 and GEM-TC2020 products.

Of the 101 points showing clear agreement, 30 (30%) were commission-type mismatches and 71 (70%) were omission-type mismatches. The main sources of these mismatches were sparse or scattered woody vegetation and shrub-tree confusion (58%), forest edge or transitional zones (32%), with smaller contributions from land-use vs. land-cover inconsistencies. The identified OEs



460 were spatially concentrated along forest boundaries and in areas with gradual canopy transitions, rather than within homogeneous core forest or clearly non-forested regions.

Overall, most disagreements in the GEM-FnF2020 map arise from transitional or ambiguous land-cover types, which pose inherent challenges for the AEF vector space in distinguishing forest and non-forest, consistent with previous EO-based global forest mapping approaches (Bourgoin et al., 2026; Neumann et al., 2025; Shimada et al., 2014; Xiao et al., 2024). Sparse or scattered 465 woody vegetation, shrub-tree mosaics, and forest edges account for the majority of errors, while land use conflicts and differences in forest definitions could explain the remaining errors. Disagreements are concentrated in open boreal forests, tropical savanna mosaics and fragmented agricultural landscapes. Up to 28% of identified OEs and CEs may reflect correct classifications, indicating that the actual accuracy of GEM-FnF2020 is likely higher than suggested by comparison with the main validation dataset.

3.6 Comparison of the GEM-FnF2020 and the tree crop class quality with other global forest maps

470 In comparison to other global F/nF datasets, based on the main validation dataset, our SVM-based GEM-FnF2020 map ranks second in OA, with differences of 1.2% in OA, and 0.015 in macro F1-score, compared to the JRC's GFC2020 v3 dataset (Figure 7). The GFC2020 v2 achieved a very similar, but slightly lower OA than our GEM-FnF2020 map, with macro F1-scores of 0.90. The other F/nF datasets achieved relatively high and comparable overall accuracies on the main validation dataset, with OA ranging from 85% to 90% and macro F1-scores from 0.83 to 0.89. Regarding error rates, our dataset achieves balanced OE and CE rates for the forest 475 class, at 15.28% and 12.73%, respectively, which are comparable to the GFC2020 v3 error rates of 10.84% and 12.63%. In contrast, the other F/nF datasets show higher bias in CE compared to OE for the forest class, indicating a tendency to classify non-forest areas as forests. Higher CE rates could be related to the definition of the forest/tree cover classes in the compared datasets, as also demonstrated in the following analysis. The only exception is the IPCC dataset, which exhibits a very high OE for the forest class (28.35%) and the lowest CE of 11.50%.

480 Moderate to very high accuracies across the tree crop validation datasets were achieved by products aligned with the FAO forest definition, which excludes tree-covered areas under agricultural use. These include the GFC2020 v2/v3, IPCC, PALSAR FnF, and our GEM-FnF2020 map. Our GEM-FnF2020 product consistently ranks among the top performers, placing between first and fourth across the evaluated datasets among JRC's GFC2020 v2/v3 and IPCC (Figure 8 and Figure 9), while only our GEM-FnF2020 map and the GFC2020 v3 achieves OAs higher than 80% across all validated tree crops. Although the GFC2020 v3 product performs 485 best in most cases and the IPCC dataset achieves the highest accuracy for the European tree crop validation dataset, the absolute differences relative to our GEM-FnF2020 map are small. The PALSAR FnF product achieved moderate overall accuracies exceeding 60% for most tree crop datasets. In contrast, as expected, the lowest accuracies and highest forest commission errors (CEs), that is, points classified as forest in the products, were observed for datasets in which the forest or tree cover class effectively represents general tree cover, including perennial woody crops. The CGLCL and ESA WorldCover datasets, where tree crops are 490 classified as forest/tree cover (see (Buchhorn et al., 2020) and (Van De Kerchove et al., 2020), respectively) achieved the lowest accuracies (3-30%) and the highest shares of forest CEs (above 80%) for all datasets except European tree crops. The Hansen et al.'s GFC product also represents tree cover rather than forest according to the FAO definition. Although this distinction was not



explicitly stated in the original publication or its supplementary materials (Hansen et al., 2013), it has been highlighted by the research community directly after its publication (Tropek et al., 2014) or recently in (Freitas Beyer et al., 2025). Consequently, GFC also performed poorly in terms of overall accuracy and forest CE across most tree crop validation datasets, with CE values exceeding 40%.

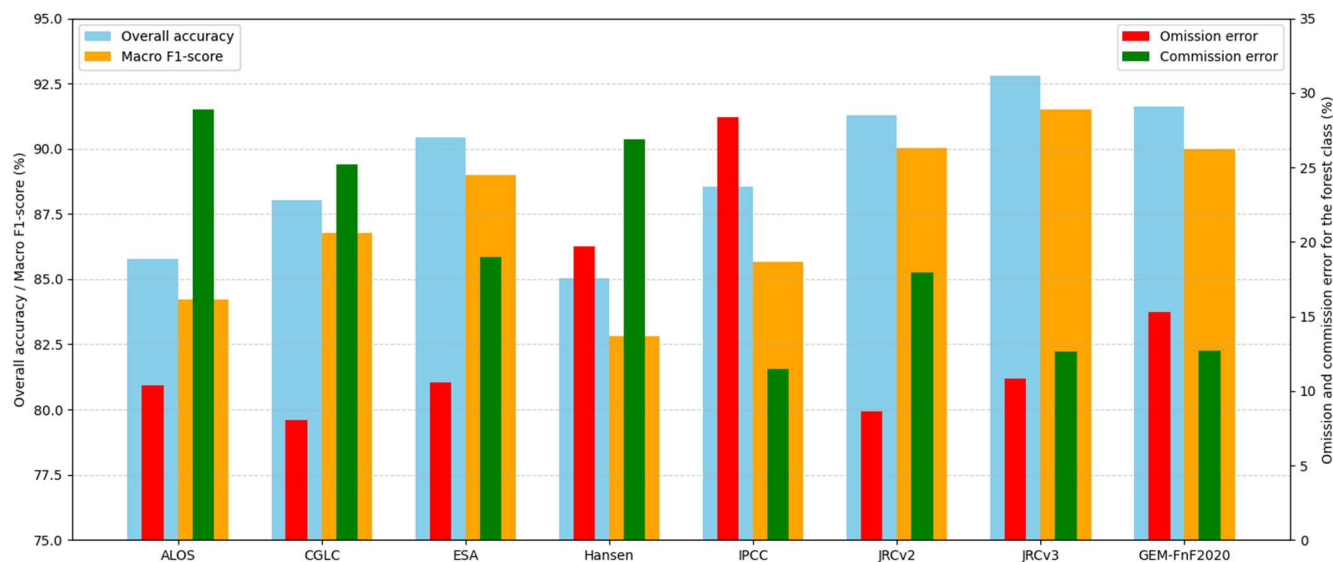


Figure 7. Comparison of OA, macro F1-score and OE and CE for the forest class among global F/nF products and our SVM-based GEM-FnF2020 map.

500

It should be noted that both the GFC2020 and IPCC products, which outperform our GEM-FnF2020 map for selected tree crop types, were created by compositing multiple input datasets. The IPCC dataset combines various land use, land cover, and forest parameter products through Boolean analysis (Hunka et al., 2024b), while the GFC2020 products integrate numerous global and regional land cover, forest, and plantation datasets together with additional thematic layers, with plantation areas explicitly masked and reclassified as non-forest (Bourgoin et al., 2026). As a result, they are highly optimized for a specific reference period and can achieve superior performance, but their application for different years requires updated ancillary inputs. Moreover, their quality and spatial resolution are limited by the characteristics of the underlying input datasets.

505

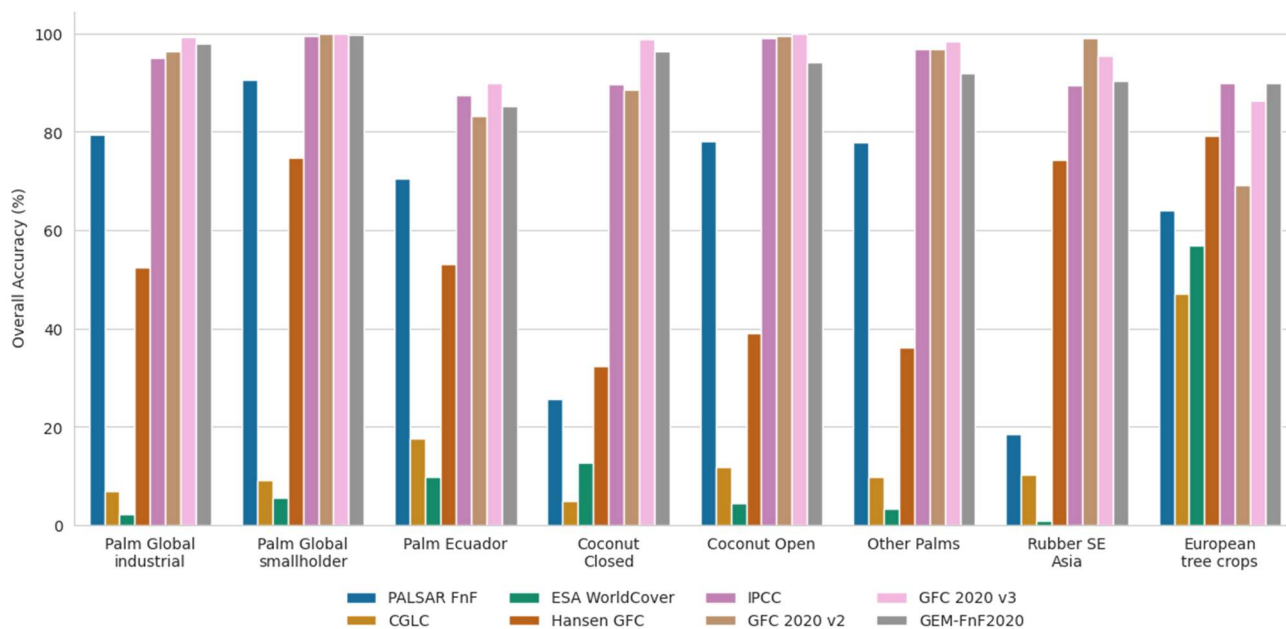
In contrast, our embedding-based approach enables consistent multi-year mapping using efficient and transparent machine learning methods, which is critical for monitoring applications such as deforestation assessment, carbon accounting and land use change analysis. Notably, the automatic training procedure in our approach, that is based on strict forest, non-forest and tree crop masks, helps to mitigate the limitations of individual input datasets, although some outlier forest, non-forest, or tree crop samples may still be included in the training data. As an additional contribution, we provide the trained model weights that allow users to generate F/nF and F/nF/tree crop maps for the period 2017–2025, when AEF embeddings are available. Importantly, our product performs best among datasets derived solely from EO data, highlighting the effectiveness of the proposed automatic training data generation and classification framework without reliance on external thematic inputs.

510

515



Overall, the results demonstrate that while composite products currently achieve the highest absolute accuracy with the lowest forest CEs, EO-driven approaches, such as the novel GEM-FnF2020 map, present an attractive alternative due to their competitive performance combined with methodological transparency and temporal scalability.



520 **Figure 8.** Accuracy of classifying tree crop areas as non-forest in global FnF products and SVM-based GEM-FnF2020, based on tree crop validation datasets.

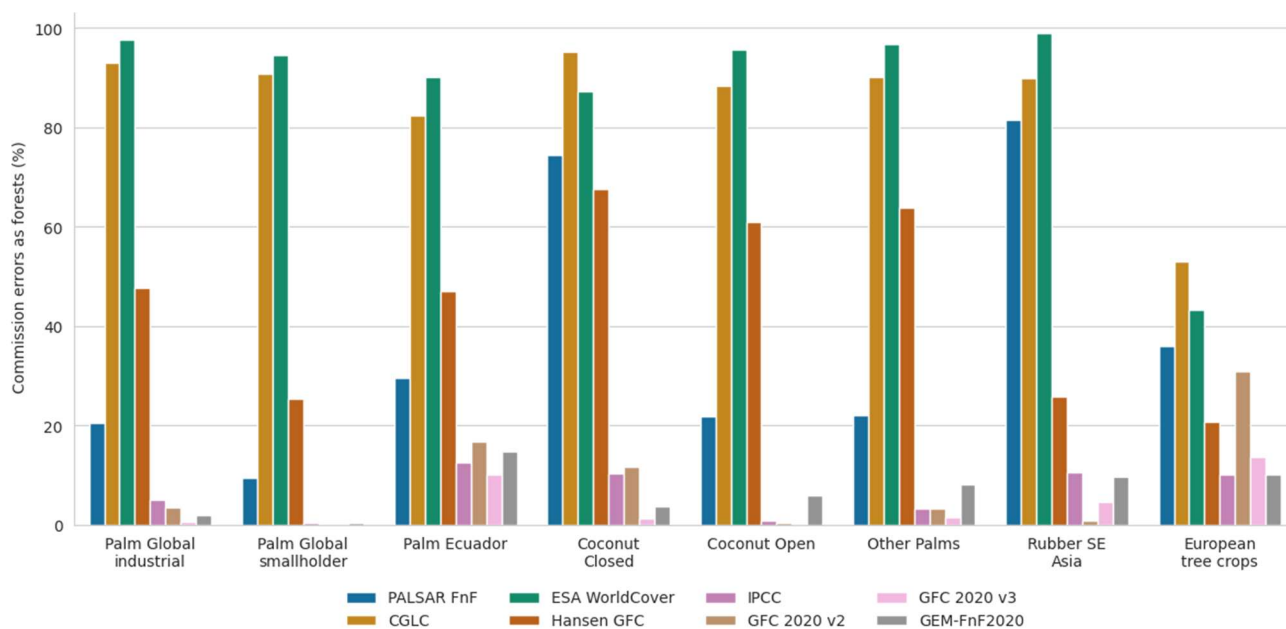


Figure 9. Rates of misclassification of plantation areas as forests (forest CEs) for the selected global FnF datasets and SVM-based GEM-FnF2020, based on tree crop validation datasets.



525 3.7 Implications for global forest mapping

Overall, these results demonstrate that AEF embeddings provide a highly informative and transferable representation for global F/nF and tree crop mapping. Their effectiveness across instance-based, linear and non-linear models confirms that much of the relevant information for forest discrimination is already encoded in the embedding space. This supports the use of simple, transparent classifiers for large-scale and multi-temporal forest monitoring.

530 At the same time, confusion between forests and certain tree crops highlights a fundamental challenge for global forest mapping. While AEF embeddings substantially improve separability compared to raw spectral inputs, further gains will likely require additional and more specific training data for specific tree crops, more contextual information, such as temporal dynamics, spatial context or region-specific calibration, rather than increased classifier complexity alone. In this direction, our dataset is a first effort in this direction, on the one hand showing the capabilities of AEF embeddings, on the other, showing the need of better data to get
535 better results.

Our GEM-FnF2020 map achieves comparable overall accuracy on the main F/nF validation dataset and on tree crop validation datasets relative to the best-performing GFC2020 v3 product. Its primary advantage, however, lies in its straightforward transferability to other years for which AEF embeddings are available or will become available (currently 2017–2025). In contrast, composite products such as GFC2020 v3 would require updated ancillary input layers to be reproduced for additional time periods.

540 In light of policy regulations such as the EUDR and other national strategies, the presented GEM-Forest dataset and its potential future multi-temporal extensions can support deforestation assessment and other decision-making processes by users and policy-makers, alongside other global or more detailed regional products (not limited to EO-based data), ground-based observations or references, as highlighted in van Noordwijk et al. (2025).

3.8 Limitations

545 Despite the high potential for reproducibility of the GEM-Forest dataset for years other than 2020, and thus its potential use for change detection analyses, an important limitation remains: the GEM-Forest dataset and its derived products can only be generated for years in which AEF satellite embeddings are available, currently 2017–2025. Commission errors in the forest class of the GEM-FnF2020 product occur in some urban areas where the combined GUB GAIA and FADSL datasets do not fully capture the extent of urban land cover. It should also be noted that GEM-Forest does not explicitly account for clear-cut areas where forest regrowth
550 is expected in the future, as such areas are classified as forest under both FAO and EUDR forest definitions.

The tree crop classes used in the training process include oil palm, rubber, coconut, and European tree crops, specifically fruit trees and olive orchards; therefore, the GEM-TC2020 product primarily reflects these classes. It should be noted that cocoa and coffee plantations were not used in the training process due to the lack of high quality open-access global cocoa or coffee datasets and the absence of reliable validation datasets. Moreover, cocoa cultivation often occurs beneath the canopy of other trees, which makes the
555 distinction between cocoa plantations and natural tree cover difficult using EO data. For example, full-sun (non-shaded) cocoa plantations, those that could be reliably monitored by EO-based data, represent only about 9% and 25% of cocoa systems in



Nicaragua and Peru, respectively (Orozco-Aguilar et al., 2021). Even in Ghana and Côte d'Ivoire, where over 80% share of full-sun and close to full-sun cocoa plantations were reported (Becker et al., 2025), existing EO-based studies (Abu et al., 2021) report limited performance in cocoa mapping, with low OEs but moderate CEs (17% and 38%, respectively). Similarly, the coffee probability dataset from the Forest Data Partnership shows a trade-off between OE and CE only at around 54% (Forest Data Partnership, 2025). Initial tests incorporating coffee and cocoa probability layers from this dataset did not yield satisfactory results and increased OE for the forest class. Therefore, cocoa and coffee were excluded from the training process.

Low error rates in forest classification over tree crop areas were observed based on the eight tree crop validation datasets. However, additional validation datasets would allow a more comprehensive assessment of the tree crop class and could help identify the main problematic regions, while it could support further improvement of the GEM-Forest dataset. Based on qualitative evaluation, tree crop areas seem underrepresented in some regions and overrepresented in others. The most challenging areas occur in small-scale, fragmented tree crop landscapes, particularly in Europe, where the lowest OAs were recorded. In these regions, most tree crop omission errors correspond to areas classified as non-forest and indicates that the trained ML models demonstrate limited ability to reliably distinguish between non-forest and European tree crop systems.

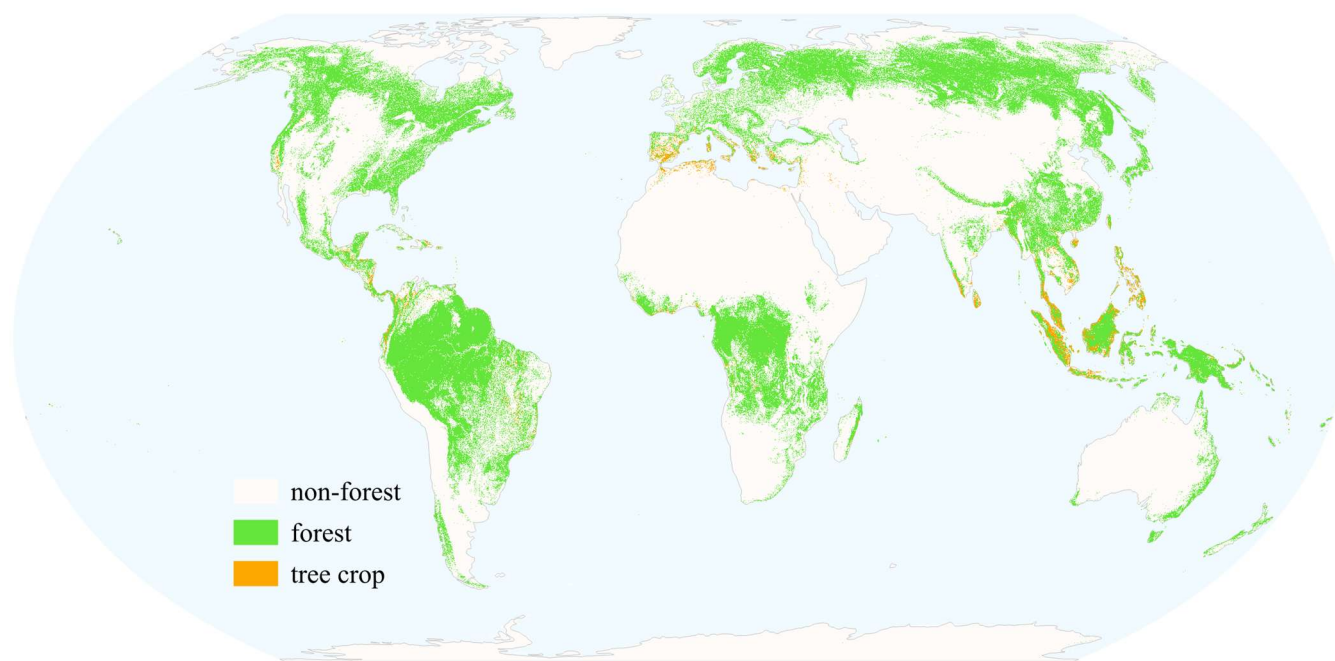


Figure 10. Global forest and tree crop extent based on GEM-Forest for 2020 in a 500 m/pixel aggregation, visualised in the Equal Earth projection (EPSG:8857).

Data availability

The GEM-Forest products, GEM-FnF2020 and GEM-TC2020 can be accessed through the GEE application online, via the following URL: danielp-cuni.projects.earthengine.app/view/gem-forest. The GEM-Forest dataset for 2020 is being gradually



uploaded to the following Zenodo repository: <http://doi.org/10.5281/zenodo.18921586> (as of 12.03.2026, available in a preview mode through this link:

<https://zenodo.org/records/18921586?preview=1&token=eyJhbGciOiJIUzUxMiJ9.eyJpZCI6ImYxNGM0ZWl4LWY2OGYtNDlmOC1hMTUw>

580

[LThkODRhNWQ0OTk0YSIsImRhGEiOnt9LCJyYW5kb20iOiI3ZTY2MTQxNTZmNmJmJmEYMGFkNDVhOTI4MjM2NlMSJ9.199SnzdIKByVuE8v1_908aJzYB9DqLjGCwzv0taD0nvHrpKBeP5X3xIOSscHP_m0WFE1hO5flicKRE2kJFYeiQ](https://zenodo.org/records/18921586?preview=1&token=eyJhbGciOiJIUzUxMiJ9.eyJpZCI6ImYxNGM0ZWl4LWY2OGYtNDlmOC1hMTUwLThkODRhNWQ0OTk0YSIsImRhGEiOnt9LCJyYW5kb20iOiI3ZTY2MTQxNTZmNmJmJmEYMGFkNDVhOTI4MjM2NlMSJ9.199SnzdIKByVuE8v1_908aJzYB9DqLjGCwzv0taD0nvHrpKBeP5X3xIOSscHP_m0WFE1hO5flicKRE2kJFYeiQ)). This repository also includes the training and validation datasets with AEF embedding vector values which were used in the training and validation of the ML models, and the saved classification weights for RR, LR, SVM, RF, XGBoost, MLP₁₀ and MLP₁₀₀.

Code availability

585

All the supporting codes to generate the training areas, training data, ML models training and testing, and for the reimplementation of the SVM weights to GEE will be made publicly available after the review process on GitHub: github.com/palubad/GEM-Forest. The supporting codes for pre-review access are available from the corresponding author on reasonable request.

4. Conclusions

590

Overall, these results demonstrate that AEF embeddings provide a highly informative and transferable representation for global F/nF mapping, as evidenced by the global GEM-Forest dataset with its GEM-FnF2020 and GEM-TC2020 maps at 10 m spatial resolution. We show that simple, resource-efficient linear ML approaches combined with AEF can produce highly accurate global F/nF maps, often outperforming more complex algorithms. Moreover, the tree crop class within GEM-TC2020 shows good performance in delineating tree crops and further confirms the low misclassification rates of plantations as forests.

595

The proposed approach shows strong potential for transfer across the 2017–2024 period, which enables multi-year applications based on models trained for a single year and represents a key next step in our research. We further demonstrate that the inclusion of training data representing tree crops substantially improves product quality and supports the exclusion of tree-covered agricultural areas from the forest class. In addition, reliance on a single global F/nF validation dataset has clear limitations; we therefore recommend the inclusion of complementary thematic validation datasets to better capture common classification challenges, particularly the confusion between forests and tree crops or plantations. The main limitations of AEF are its annual temporal resolution, which prevents near-real-time or intra-annual applications, and the limited interpretability of the embedding features in downstream analyses.

600

These results and the presented approach can support policy and regulatory applications, including the EUDR, while the open-access release of datasets and trained models facilitates global use, further evaluation, and methodological development by the EO and forest monitoring communities.



605 Appendices

Appendix A. Description of the methodology used for the generation of the validation dataset of the European tree crops (fruit and olive orchards)

The CORINE Land Cover 2018 (CLC2018) dataset was used to construct an independent validation dataset for assessing the accuracy of the tree crop class in the GEM-TC2020 map over Europe. Two CLC classes representing permanent tree crops were selected: fruit trees and berry plantations (class 222) and olive groves (class 223). To ensure spatial relevance and reduce the influence of very small or potentially mixed land cover patches, only polygons with a minimum area of 25 ha were retained for further analysis.

Following this filtering step, a stratified point sampling strategy was applied to generate validation points while accounting for the wide range of polygon sizes. Polygons were grouped into size classes, and the number of validation points assigned to each group was proportional to polygon area in order to better represent large and spatially heterogeneous plantations, while avoiding over-representation of small polygons. The sampling strategy was defined as follows:

- Polygons with an area between 25 ha and 10,000 ha (40,843 polygons): a total of 100 validation points were randomly distributed across this group.
- Polygons with an area between 10,000 ha and 20,000 ha (50 polygons): two validation points were generated per polygon, resulting in 100 points.
- Polygons with an area between 20,000 ha and 50,000 ha (25 polygons): three validation points were generated per polygon, resulting in 75 points.
- Polygons with an area between 50,000 ha and 100,000 ha (7 polygons): four validation points were generated per polygon, resulting in 28 points.

In total, 303 validation points were generated across Europe. All points were subsequently visually interpreted using high-resolution satellite imagery available in Google Earth Pro, with particular attention to the temporal consistency of tree crop presence around the reference year 2020. Points located in areas showing land cover change, mixed land use, or ambiguous tree crop patterns were excluded to ensure a high-confidence validation dataset. During this final validation step, 9 points were excluded because it was not possible to unambiguously determine whether the land cover represented a tree crop plantation or another type of woody or mixed vegetation. The final CORINE-based validation dataset therefore consisted of 294 high-confidence validation points.

635

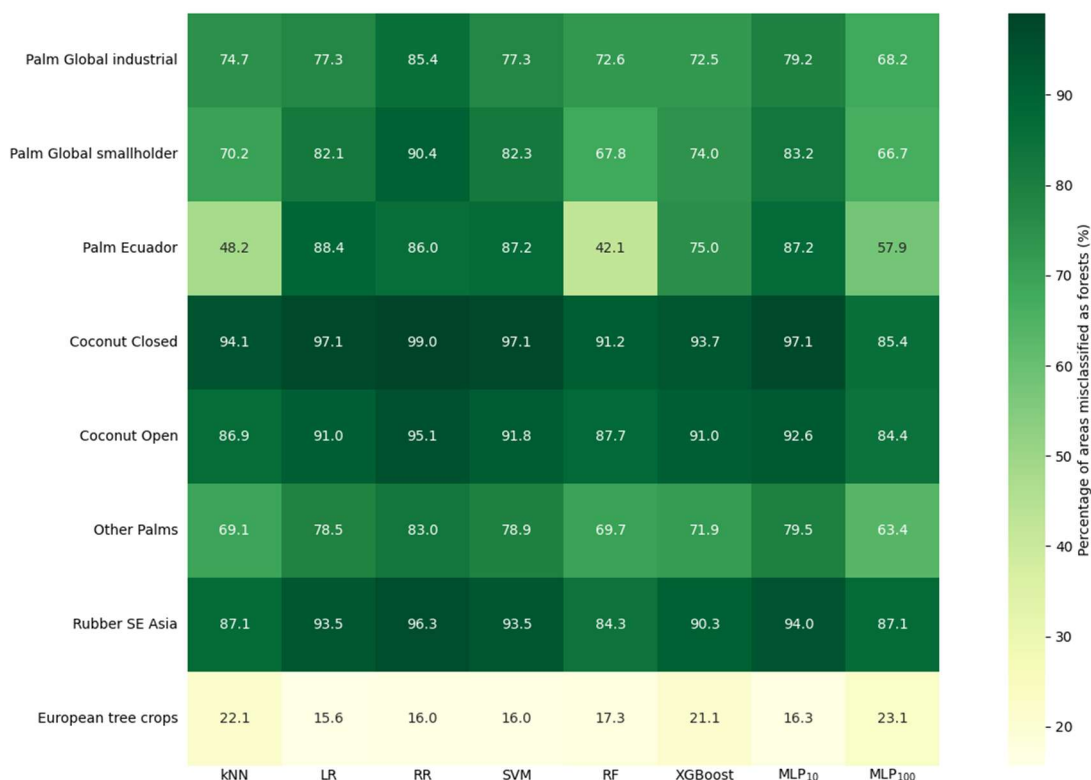


Appendix B. Accuracy metrics for the F/nF classification where only forest and non-forest training samples were used to train the ML models.

Model	OA	macro-F1*100	w-F1*100	OE	CE	OE F	CE F	OE nF	CE nF
KNN	91.13	89.59	91.16	10.18	10.63	13.54	15.30	6.82	91.13
LR	91.97	90.51	91.97	9.48	9.50	13.16	13.24	5.79	91.97
RR	91.62	89.98	91.57	10.45	9.54	15.72	12.33	5.18	91.62
SVM	91.95	90.52	91.96	9.33	9.62	12.60	13.70	6.06	91.95
RandomForest									
RF	91.50	89.82	91.44	10.75	9.55	16.51	12.04	4.99	91.50
XGBoost	91.63	90.10	91.62	9.95	9.85	13.97	13.61	5.92	91.63
MLP ₁₀	91.93	90.52	91.95	9.27	9.69	12.33	13.95	6.21	91.93
MLP ₁₀₀	92.11	90.69	92.12	9.25	9.36	12.72	13.16	5.78	92.11

Appendix C. Percentage of areas misclassified as forest class (forest CEs) based on the tree crop validation datasets for the F/nF classification where only forest and non-forest training samples were used to train the ML models.

640





Appendix D. Mean overall accuracy, mean commission errors for the tree crop validation datasets and mean overall accuracy when tree crops (TC) were merged to the non-forest (nF) class. Bolded results represent the best achieved accuracies, while SVM (underscored) was selected for further evaluation.

Model	OA	CE as F	CE as nF	OA (TC as nF)
KNN	80.80	6.66	12.54	93.34
LR	78.84	7.51	13.65	92.49
RR	78.45	9.58	11.96	90.42
<u>SVM</u>	<u>77.80</u>	<u>7.14</u>	<u>15.06</u>	<u>92.86</u>
RF	66.11	14.24	19.65	85.76
XGBoost	71.43	12.64	15.93	87.36
MLP ₁₀	77.07	8.59	14.34	91.41
MLP ₁₀₀	75.45	8.29	16.25	91.71

645 Author contribution

D.P. and A.H. conceived and designed the study and its methodology, A.H. supervised the study, D.P. and V.M. conducted the experiments, performed the analysis and prepared the supporting codes. D.P. lead the data curation, manuscript preparation and validation of the results. K.O. and Y.T.P.Q. contributed to data curation and validation of the results. All authors contributed to manuscript review and editing and approved the final manuscript.

650 Competing interests

The authors declare that they have no conflict of interest.

Financial support

This research was supported by the Johannes Amos Comenius Programme (P JAC), project No. CZ.02.01.01/00/22_008/0004605, Natural and anthropogenic georisks. AH & YTPQ also acknowledge funding from Charles University PRIMUS programme (PRIMUS/23/SCI/013), the Grant Agency of Charles University (GAUK), project no. [448325], and the Charles University Research Centre programme (UNCE/24/SCI/006). This research was also supported by the Slovak Research and Development Agency (APVV) under contract No. APVV-23-0210: Urban Overheating: Consequences, Mitigation and Perception, and by the Cultural and Educational Grant Agency of the Ministry of Education, Science, Research and Sport of the Slovak Republic (KEGA) under contract No. KEGA 023UPJŠ-4/2025: Remote Sensing Education with a Focus on Satellite and Unmanned Aerial Platforms

660 – Development of a Textbook and Online Educational Resources.



Acknowledgements

This publication has been prepared using European Union's Copernicus Land Monitoring Service information; specifically the Forest Additional Support Layer (FADSL) from the High Resolution Layer Tree Cover and Forests product, DOI: <https://doi.org/10.2909/4605463b-7150-49c6-9b45-01bf542891a9>. We would like to thank Maxim Neumann and Yuchang Jiang for providing early access to their 10 m-resolution tree crop map of South America from (Jiang et al., . (2026). We would also like to thank Jakub Lysák and Hugo Majer for their useful suggestions.

References

Abu, I.-O., Szantoi, Z., Brink, A., Robuchon, M., and Thiel, M.: Detecting cocoa plantations in Côte d'Ivoire and Ghana and their implications on protected areas, *Ecol. Indic.*, 129, 107863, <https://doi.org/10.1016/j.ecolind.2021.107863>, 2021.

670 Ball, J. G., Wicklein, J. A., Feng, Z., Knezevic, J., Jaffer, S., Atzberger, C., Dalponte, M., and Coomes, D.: Geospatial foundation models enable data-efficient tree species mapping in temperate montane forests, <https://doi.org/10.64898/2026.02.23.707022>, 2026.

Bartels, S. F., Chen, H. Y. H., Wulder, M. A., and White, J. C.: Trends in post-disturbance recovery rates of Canada's forests following wildfire and harvest, *For. Ecol. Manag.*, 361, 194–207, <https://doi.org/10.1016/j.foreco.2015.11.015>, 2016.

675 Becker, A., Wegner, J. D., Dawoe, E., Schindler, K., Thompson, W. J., Bunn, C., Garrett, R. D., Castro-Llanos, F., Hart, S. P., and Blaser-Hart, W. J.: The unrealized potential of agroforestry for an emissions-intensive agricultural commodity, *Nat. Sustain.*, 8, 994–1003, <https://doi.org/10.1038/s41893-025-01608-7>, 2025.

Bourgoin, C., Verhegghen, A., Carboni, S., Ameztoy, I., Ceccherini, G., Colditz, R., and Achard, F.: Global map of forest types 2020 - version 0 (version 0), <http://data.europa.eu/89h/037ca376-ba92-49db-a8f7-0c277c1e5436>, 2024.

680 Bourgoin, C., Verhegghen, A., Carboni, S., Degreve, L., Ameztoy, I., Ceccherini, G., Colditz, R., and Achard, F.: Global forest maps for the year 2020 to support the EU regulation on deforestation-free supply chains: improved map of global forest cover(GFC2020) and preliminary map of global forest types (GFT2020)., Publications Office, LU, <https://doi.org/10.2760/1975879>, 2025.

Bourgoin, C., Verhegghen, A., Carboni, S., Ameztoy, I., Degreve, L., Fritz, S., Herold, M., Tsendbazar, N., Lesiv, M., Achard, F., and Colditz, R.: GFC2020: a global map of forest land use for year 2020 to support the EU Deforestation Regulation, *Earth Syst. Sci. Data*, 18, 1331–1365, <https://doi.org/10.5194/essd-18-1331-2026>, 2026.

685 Brown, C. F., Kazmierski, M. R., Pasquarella, V. J., Rucklidge, W. J., Samsikova, M., Zhang, C., Shelhamer, E., Lahera, E., Wiles, O., Ilyushchenko, S., Gorelick, N., Zhang, L. L., Alj, S., Schechter, E., Askay, S., Guinan, O., Moore, R., Boukouvalas, A., and Kohli, P.: AlphaEarth Foundations: An embedding field model for accurate and efficient global mapping from sparse label data, <https://doi.org/10.48550/arXiv.2507.22291>, 29 July 2025.

690 Buchhorn, M., Smets, B., Bertels, L., Roo, B. D., Lesiv, M., Tsendbazar, N.-E., Li, L., and Tarko, A.: Copernicus Global Land Service: Land Cover 100m: version 3 Globe 2015-2019: Product User Manual, Zenodo, <https://doi.org/10.5281/ZENODO.3938963>, 2020.



- Bunting, P., Rosenqvist, A., Hilarides, L., Lucas, R. M., Thomas, N., Tadono, T., Worthington, T. A., Spalding, M., Murray, N. J., and Rebelo, L.-M.: Global Mangrove Extent Change 1996–2020: Global Mangrove Watch Version 3.0, *Remote Sens.*, 14, 3657, 695 <https://doi.org/10.3390/rs14153657>, 2022a.
- Bunting, P., Rosenqvist, A., Hilarides, L., Lucas, R., Thomas, N., Tadono, T., Worthington, T., Spalding, M., Murray, N., and Rebelo, L.-M.: Global Mangrove Watch (1996 - 2020) Version 3.0 Dataset (3.0), <https://doi.org/10.5281/ZENODO.6894273>, 2022b.
- Chen, T. and Guestrin, C.: XGBoost: A Scalable Tree Boosting System, in: Proceedings of the 22nd ACM SIGKDD International Conference on Knowledge Discovery and Data Mining, 785–794, <https://doi.org/10.1145/2939672.2939785>, 2016.
- Clinton, N., Vollrath, A., D’annunzio, R., Liu, D., Glick, H. B., Descals, A., Sullivan, A., Guinan, O., Abramowitz, J., Stolle, F., Goodman, C., Birch, T., Quinn, D., Danylo, O., Lips, T., Coelho, D., Bihari, E., Cronkite-Ratcliff, B., Poortinga, A., Haghigattalab, A., Notman, E., DeWitt, M., Yonas, A., Donchyts, G., Shah, D., Saah, D., Tenneson, K., Quyen, N. H., Verma, M., and Wilcox, A.: A community palm model, <https://doi.org/10.48550/arXiv.2405.09530>, 20 November 2024.
- 705 Colditz, R., Verhegghen, A., Carboni, S., Bourgoïn, C., and Achard, F.: Validation dataset for the global map of forest cover 2020 - version 2 (2), 2025.
- Cook-Patton, S. C., Leavitt, S. M., Gibbs, D., Harris, N. L., Lister, K., Anderson-Teixeira, K. J., Briggs, R. D., Chazdon, R. L., Crowther, T. W., Ellis, P. W., Griscom, H. P., Herrmann, V., Holl, K. D., Houghton, R. A., Larrosa, C., Lomax, G., Lucas, R., Madsen, P., Malhi, Y., Paquette, A., Parker, J. D., Paul, K., Routh, D., Roxburgh, S., Saatchi, S., van den Hoogen, J., Walker, W. 710 S., Wheeler, C. E., Wood, S. A., Xu, L., and Griscom, B. W.: Mapping carbon accumulation potential from global natural forest regrowth, *Nature*, 585, 545–550, <https://doi.org/10.1038/s41586-020-2686-x>, 2020.
- Copernicus Land Monitoring Service: Land Cover 2015-2019 (raster 100 m), global, annual - version 3 (3.0), <https://doi.org/10.2909/C6377C6E-76CC-4D03-8330-628A03693042>, 2015.
- Descals, A.: High-resolution global map of closed-canopy coconut palm (v1-2), <https://doi.org/10.5281/ZENODO.8128183>, 2023.
- 715 Descals, A.: Global oil palm extent and planting year from 1990 to 2021, <https://doi.org/10.5281/zenodo.13379129>, 2024a.
- Descals, A.: Validation dataset for the article “Rubber planting and deforestation,” <https://doi.org/10.5281/zenodo.10646349>, 2024b.
- Descals, A., Wich, S., Szantoi, Z., Struebig, M. J., Dennis, R., Hatton, Z., Ariffin, T., Unus, N., Gaveau, D. L. A., and Meijaard, E.: High-resolution global map of closed-canopy coconut palm, *Earth Syst. Sci. Data*, 15, 3991–4010, <https://doi.org/10.5194/essd-15-3991-2023>, 2023.
- 720 Descals, A., Gaveau, D. L. A., Wich, S., Szantoi, Z., and Meijaard, E.: Global mapping of oil palm planting year from 1990 to 2021, *Earth Syst. Sci. Data*, 16, 5111–5129, <https://doi.org/10.5194/essd-16-5111-2024>, 2024.
- Dinerstein, E., Olson, D., Joshi, A., Vynne, C., Burgess, N. D., Wikramanayake, E., Hahn, N., Palminteri, S., Hedao, P., Noss, R., Hansen, M., Locke, H., Ellis, E. C., Jones, B., Barber, C. V., Hayes, R., Kormos, C., Martin, V., Crist, E., Sechrest, W., Price, L., 725 Baillie, J. E. M., Weeden, D., Suckling, K., Davis, C., Sizer, N., Moore, R., Thau, D., Birch, T., Potapov, P., Turubanova, S., Tyukavina, A., de Souza, N., Pintea, L., Brito, J. C., Llewellyn, O. A., Miller, A. G., Patzelt, A., Ghazanfar, S. A., Timberlake, J.,



Klöser, H., Shennan-Farpón, Y., Kindt, R., Lillesø, J.-P. B., van Breugel, P., Graudal, L., Voge, M., Al-Shammari, K. F., and Saleem, M.: An Ecoregion-Based Approach to Protecting Half the Terrestrial Realm, *BioScience*, 67, 534–545, <https://doi.org/10.1093/biosci/bix014>, 2017.

730 European Environment Agency: CORINE Land Cover 2018 (vector), Europe, 6-yearly (20.01), <https://doi.org/10.2909/71C95A07-E296-44FC-B22B-415F42ACFDf0>, 2020.

European Environment Agency: Forest Additional Support Layer 2018 - Present (raster 10m), Europe, 3-yearly, Nov. 2024 (01.00), <https://doi.org/10.2909/4605463B-7150-49C6-9B45-01BF542891A9>, 2024.

FAO: FAO GAUL: Global Administrative Unit Layers 2015, Country Boundaries, 2015.

735 FAO: The State of the World's Forests 2022, FAO, <https://doi.org/10.4060/cb9360en>, 2022.

FAO: Global Forest Resources Assessment - FRA 2025 - Terms and Definitions, 2023.

Feng, Z., Atzberger, C., Jaffer, S., Knezevic, J., Sormunen, S., Young, R., Lisaius, M. C., Immitzer, M., Jackson, T., Ball, J., Coomes, D. A., Madhavapeddy, A., Blake, A., and Keshav, S.: TESSERA: Temporal Embeddings of Surface Spectra for Earth Representation and Analysis, <https://doi.org/10.48550/ARXIV.2506.20380>, 2025.

740 Forest Data Partnership: Community models 2025a, 2025.

Forgaard, T., Reksten, J. H., Waldeland, A. U., Marsocci, V., Longépé, N., Kampffmeyer, M., and Salberg, A.-B.: THOR: A Versatile Foundation Model for Earth Observation Climate and Society Applications, <https://doi.org/10.48550/ARXIV.2601.16011>, 2026.

Forzieri, G., Dakos, V., McDowell, N. G., Ramdane, A., and Cescatti, A.: Emerging signals of declining forest resilience under climate change, *Nature*, 608, 534–539, <https://doi.org/10.1038/s41586-022-04959-9>, 2022.

745 Freitas Beyer, J., Köthke, M., and Lippe, M.: Assessing the Suitability of Available Global Forest Maps as Reference Tools for EUDR-Compliant Deforestation Monitoring, *Remote Sens.*, 17, 3012, <https://doi.org/10.3390/rs17173012>, 2025.

Fundación EcoCiencia: Documento de validación: “Machine Learning Training Data for Continental Ecuador and Galapagos from 1985 to 2023” (v1.0), 2025.

750 Gao, X., Pasquarella, V., Laflower, D., and Thompson, J. R.: Mapping Forest Communities, Including Species Composition, Structure, and Carbon, at 10-m Resolution Using Geospatial Embeddings, <https://doi.org/10.2139/ssrn.5936862>, 18 December 2025.

Gorelick, N., Hancher, M., Dixon, M., Ilyushchenko, S., Thau, D., and Moore, R.: Google Earth Engine: Planetary-scale geospatial analysis for everyone, *Remote Sens. Environ.*, 202, 18–27, <https://doi.org/10.1016/j.rse.2017.06.031>, 2017.

755 Hansen, M. C., Potapov, P. V., Moore, R., Hancher, M., Turubanova, S. A., Tyukavina, A., Thau, D., Stehman, S. V., Goetz, S. J., Loveland, T. R., Kommareddy, A., Egorov, A., Chini, L., Justice, C. O., and Townshend, J. R. G.: High-Resolution Global Maps of 21st-Century Forest Cover Change, *Science*, 342, 850–853, <https://doi.org/10.1126/science.1244693>, 2013.

Hughes, A. C., Orr, M. C., Yang, Q., and Qiao, H.: Effectively and accurately mapping global biodiversity patterns for different regions and taxa, *Glob. Ecol. Biogeogr.*, 30, 1375–1388, <https://doi.org/10.1111/geb.13304>, 2021.

760 Hunka, N., Duncanson, L., Armston, J., Dubayah, R. O., Healey, S. P., Santoro, M., May, P. B., Araza, A., Bourgain, C., Montesano, P. M., Neigh, C. S., Grantham, H., Potapov, V., Turubanova, S., Tyukavina, A., Richter, J., Harris, N., Urbazaev, M., Pascual, A.,



Requena Suarez, D., Herold, M., Poulter, B., Wilson, S. N., Grassi, G., Federici, S., Sanz Sanchez, M. J., and Melo, J.: Carbon Monitoring System (CMS) Classification of Global Forests for IPCC Aboveground Biomass Tier 1 Estimates, 2020, <https://doi.org/10.3334/ORNLDAAC/2345>, 1 January 2024a.

765 Hunka, N., Duncanson, L., Armston, J., Dubayah, R., Healey, S. P., Santoro, M., May, P., Araza, A., Bourgoin, C., Montesano, P., M., Neigh, C. S. R., Grantham, H., Potapov, P., Turubanova, S., Tyukavina, A., Richter, J., Harris, N., Urbazaev, M., Pascual, A., Suarez, D. R., Herold, M., Poulter, B., Wilson, S. N., Grassi, G., Federici, S., Sanz, M. J., and Melo, J.: Intergovernmental Panel on Climate Change (IPCC) Tier 1 forest biomass estimates from Earth Observation, *Sci. Data*, 11, 1127, <https://doi.org/10.1038/s41597-024-03930-9>, 2024b.

770 Jakubik, J., Yang, F., Blumenstiel, B., Scheurer, E., Sedona, R., Maurogiovanni, S., Bosmans, J., Dionelis, N., Marsocci, V., Kopp, N., Ramachandran, R., Fraccaro, P., Brunschwiler, T., Cavallaro, G., Bernabe-Moreno, J., and Longépé, N.: TerraMind: Large-Scale Generative Multimodality for Earth Observation, <https://doi.org/10.48550/ARXIV.2504.11171>, 2025.

Jiang, Y., Raichuk, A., Tong, X., Garnot, V. S. F., Ortiz-Gonzalo, D., Morris, D., Schindler, K., Wegner, J. D., and Neumann, M.: Tree crop mapping of South America reveals links to deforestation and conservation, <https://doi.org/10.48550/arXiv.2602.17372>, 24 February 2026.

775 Lesiv, M., Schepaschenko, D., Buchhorn, M., See, L., Dürauer, M., Georgieva, I., Jung, M., Hofhansl, F., Schulze, K., Bilous, A., Blyshchyk, V., Mukhortova, L., Brenes, C. L. M., Krivobokov, L., Ntie, S., Tsogt, K., Pietsch, S. A., Tikhonova, E., Kim, M., Di Fulvio, F., Su, Y.-F., Zadorozhniuk, R., Sirbu, F. S., Panging, K., Bilous, S., Kovalevskii, S. B., Kraxner, F., Rabia, A. H., Vasylyshyn, R., Ahmed, R., Diachuk, P., Kovalevskyi, S. S., Bungnamei, K., Bordoloi, K., Churilov, A., Vasylyshyn, O., Sahariah, D., Tertyshnyi, A. P., Saikia, A., Malek, Ž., Singha, K., Feshchenko, R., Prestele, R., Akhtar, I. ul H., Sharma, K., Domashovets, 780 G., Spawn-Lee, S. A., Blyshchyk, O., Slyva, O., Ilkiv, M., Melnyk, O., Sliusarchuk, V., Karpuk, A., Terentiev, A., Bilous, V., Blyshchyk, K., Bilous, M., Bogovyk, N., Blyshchyk, I., Bartalev, S., Yatskov, M., Smets, B., Visconti, P., Mccallum, I., Obersteiner, M., and Fritz, S.: Global forest management data for 2015 at a 100 m resolution, *Sci. Data*, 9, 199, <https://doi.org/10.1038/s41597-022-01332-3>, 2022.

785 Lewis, S. L., Wheeler, C. E., Mitchard, E. T. A., and Koch, A.: Restoring natural forests is the best way to remove atmospheric carbon, *Nature*, 568, 25–28, <https://doi.org/10.1038/d41586-019-01026-8>, 2019.

Li, X., Gong, P., Zhou, Y., Wang, J., Bai, Y., Chen, B., Hu, T., Xiao, Y., Xu, B., Yang, J., Liu, X., Cai, W., Huang, H., Wu, T., Wang, X., Lin, P., Li, X., Chen, J., He, C., Li, X., Yu, L., Clinton, N., and Zhu, Z.: Mapping global urban boundaries from the global artificial impervious area (GAIA) data, *Environ. Res. Lett.*, 15, 094044, <https://doi.org/10.1088/1748-9326/ab9be3>, 2020.

790 Ma, J., Li, J., Wu, W., and Liu, J.: Global forest fragmentation change from 2000 to 2020, *Nat. Commun.*, 14, 3752, <https://doi.org/10.1038/s41467-023-39221-x>, 2023.

Neumann, M., Raichuk, A., Jiang, Y., Rey, M., Stanimirova, R., Sims, M. J., Carter, S., Goldman, E., Anderson, K., Poklukar, P., Tarrío, K., Lesiv, M., Fritz, S., Clinton, N., Stanton, C., Morris, D., and Purves, D.: Natural forests of the world – a 2020 baseline for deforestation and degradation monitoring, *Sci. Data*, 12, 1715, <https://doi.org/10.1038/s41597-025-06097-z>, 2025.



- van Noordwijk, M., Dewi, S., Minang, P. A., Harrison, R. D., Leimona, B., Ekadinata, A., Burgers, P., Slingerland, M., Sassen, M.,
795 Watson, C., and Sayer, J.: Beyond imperfect maps: Evidence for EUDR-compliant agroforestry, *People Nat.*, 7, 1713–1723,
<https://doi.org/10.1002/pan3.70088>, 2025.
- Onačillová, K., Křištofová, V., and Paluba, D.: Automatic forest cover classification using Sentinel-2 multispectral satellite data
and machine learning algorithms in Google Earth Engine, *Acta Geogr. Univ. Comen.*, 67, 163–185, 2023.
- Orozco-Aguilar, L., López-Sampson, A., Leandro-Muñoz, M. E., Robiglio, V., Reyes, M., Bordeaux, M., Sepúlveda, N., and
800 Somarriba, E.: Elucidating Pathways and Discourses Linking Cocoa Cultivation to Deforestation, Reforestation, and Tree Cover
Change in Nicaragua and Peru, *Front. Sustain. Food Syst.*, 5, <https://doi.org/10.3389/fsufs.2021.635779>, 2021.
- Pedregosa, F., Varoquaux, G., Gramfort, A., Michel, V., Thirion, B., Grisel, O., Blondel, M., Prettenhofer, P., Weiss, R., Dubourg,
V., Vanderplas, J., Passos, A., Cournapeau, D., Brucher, M., Perrot, M., and Duchesnay, É.: Scikit-learn: Machine Learning in
Python, *J. Mach. Learn. Res.*, 12, 2825–2830, 2011.
- 805 Raven, P. H., Gereau, R. E., Phillipson, P. B., Chatelain, C., Jenkins, C. N., and Ulloa Ulloa, C.: The distribution of biodiversity
richness in the tropics, *Sci. Adv.*, 6, eabc6228, <https://doi.org/10.1126/sciadv.abc6228>, 2020.
- Sheil, D., Descals, A., Meijaard, E., and Gaveau, D.: Rubber planting and deforestation, *Nature*, 644, E20–E22,
<https://doi.org/10.1038/s41586-025-08848-9>, 2025.
- Shimada, M., Itoh, T., Motooka, T., Watanabe, M., Shiraiishi, T., Thapa, R., and Lucas, R.: New global forest/non-forest maps from
810 ALOS PALSAR data (2007–2010), *Remote Sens. Environ.*, 155, 13–31, <https://doi.org/10.1016/j.rse.2014.04.014>, 2014.
- Smith, C., Baker, J. C. A., and Spracklen, D. V.: Tropical deforestation causes large reductions in observed precipitation, *Nature*,
615, 270–275, <https://doi.org/10.1038/s41586-022-05690-1>, 2023.
- Tropek, R., Sedláček, O., Beck, J., Keil, P., Musilová, Z., Šimová, I., and Storch, D.: Comment on “High-resolution global maps of
21st-century forest cover change,” *Science*, 344, 981–981, <https://doi.org/10.1126/science.1248753>, 2014.
- 815 Van De Kerchove, R., Zanaga, D., Li, L., Tsendbazar, N., and Lesiv, M.: WorldCover, v1.0. Product User Manual, VITO, 2020.
- Wang, Y., Hollingsworth, P. M., Zhai, D., West, C. D., Green, J. M. H., Chen, H., Hurni, K., Su, Y., Warren-Thomas, E., Xu, J.,
and Ahrends, A.: High-resolution maps show that rubber causes substantial deforestation, *Nature*, 623, 340–346,
<https://doi.org/10.1038/s41586-023-06642-z>, 2023.
- Xiao, Y., Wang, Q., and Zhang, H. K.: Global Natural and Planted Forests Mapping at Fine Spatial Resolution of 30 m, *J. Remote*
820 *Sens.*, 4, 0204, <https://doi.org/10.34133/remotesensing.0204>, 2024.
- Xu, P., Tsendbazar, N.-E., Herold, M., De Bruin, S., Koopmans, M., Birch, T., Carter, S., Fritz, S., Lesiv, M., Mazur, E., Pickens,
A., Potapov, P., Stolle, F., Tyukavina, A., Van De Kerchove, R., and Zanaga, D.: Comparative validation of recent 10 m-resolution
global land cover maps, *Remote Sens. Environ.*, 311, 114316, <https://doi.org/10.1016/j.rse.2024.114316>, 2024.
- Zanaga, D., Van De Kerchove, R., Daems, D., De Keersmaecker, W., Brockmann, C., Kirches, G., Wevers, J., Cartus, O., Santoro,
825 M., Fritz, S., Lesiv, M., Herold, M., Tsendbazar, N.-E., Xu, P., Ramoino, F., and Arino, O.: ESA WorldCover 10 m 2021 v200
(v200), <https://doi.org/10.5281/ZENODO.7254221>, 2022.